Global and Planetary Change 158 (2017) 57–71

Contents lists available at ScienceDirect

Global and Planetary Change

journal homepage: www.elsevier.com/locate/gloplacha

Middle Miocene paleoenvironmental crises in Central Eurasia caused by changes in marine gateway configuration

Palcu D.V.[a,*], Golovina L.A.[b], Vernyhorova Y.V.[c], Popov S.V.[d], Krijgsman W.[a]

[a] Paleomagnetic Laboratory 'Fort Hoofddijk', Utrecht University, Budapestlaan 17, 3584 CD Utrecht, The Netherlands
[b] Geological Institute, Russian Academy of Sciences, Pyzhevskiy per. 7, Moscow 119017, Russia
[c] Institute of Geological Sciences, National Academy of Sciences of Ukraine, O. Honchar str., 55_b, Kyiv 01601, Ukraine
[d] Borissiak Paleontological Institute, Russian Academy of Sciences, Profsoyuznaya ul. 123, Moscow 117997, Russia

ARTICLE INFO

Keywords:
Paratethys
Middle Miocene
Biostratigraphy
Magnetostratigraphy
Extinction
Paleogeography
Chokrakian
Karaganian
Konkian
Sarmatian
Marine gateways
Straits
Black Sea

ABSTRACT

Marine gateways prove to be important factors for changes in the ecology and biochemistry of marginal seas. Changes in gateway configuration played a dominant role in the Middle Miocene paleogeographic evolution of the Paratethys Sea that covered Central Eurasia. Here, we focus on the connection between the Central (CP) and Eastern Paratethys (EP) to understand the paleoenvironmental changes caused by the evolution of this marine gateway. We first construct an integrated magneto-biostratigraphic framework for the late Langhian-Serravallian (Chokrakian-Karaganian-Konkian-Volhynian) sedimentary record of the eastern domain, which allows a correlation to the well-dated successions west of the gateway. The magneto-biostratigraphic results from the Zelensky-Panagia section on the Black Sea coast of Russia show that the Chokrakian/Karaganian boundary has an age of 13.8 Ma, the Karaganian/Konkian boundary is dated at 13.4 Ma, and the Konkian/Volhynian boundary at 12.65 Ma. We identify three major phases on gateway functioning that are reflected in specific environmental changes. During the Karaganian, the EP turned into a lake-sea that supplied a unidirectional flow of low-salinity waters to the west, where the CP sea experienced its Badenian Salinity Crisis. This configuration is remarkably similar to the Mediterranean during its Messinian Salinity Crisis. The second phase is marked by a marine transgression from the west, reinstalling open-marine conditions in the CP and causing marine incursions in the EP during the Konkian. The Volhynian is characterized by a new gateway configuration that allows exchange between CP and EP, creating unified conditions all over the Paratethys. We hypothesize that a density driven pumping mechanism is triggered by the increase in connectivity at the Konkian/Volhynian boundary, which simultaneously caused major paleoenvironmental changes at both sides of the gateway and led to the Badenian-Sarmatian extinction event in the CP.

1. Introduction

Marine gateways play a critical role in the exchange of water, heat, salt and nutrients between oceans and seas and hence impact regional and global climate. Where marine gateways link to marginal basins, the impact of hydrological exchange on the depositional environment can be profound. Even subtle changes to the hydrologic budget can alter the temperature, salinity and circulation of the marginal basin and hence transform its entire depositional environment (e.g. Bethoux and Pierre, 1999; Cramp and O'Sullivan, 1999; Flecker et al., 2015).

The Paratethys is an excellent example of a marginal basin that experienced extreme environmental crises in response to gateway evolution. During the Middle Miocene the Eastern Paratethys (Black Sea-Caspian Sea region) was connected to the open ocean via two shallow restricted gateways; the Barlad Strait to the Central Paratethys and the Trans-Tethyan gateway to the Mediterranean Sea (Popov et al., 2006, Bartol et al., 2014) (Fig. 1a). In addition, findings of polyhaline fauna in Transcaucasia and Northern Iran hint at a possible marine corridor from the South Caspian region to the Eastern Mediterranean (Popov et al., 2015). Variations in gateway configuration caused dramatic paleoceanographic events in the Central Paratethys such as marine invasions (e.g. Sant et al., 2017), huge fluctuations in salinity during the Badenian Salinity Crisis (BSC; e.g. Peryt, 2006), a major biodiversity decrease related to the Badenian Sarmatian Extinction Event (BSEE; Harzhauser and Piller, 2007) and a basin-wide change to brackish and very low salinity water conditions at the base of the regional Sarmatian and Pannonian stages, respectively (e.g. Harzhauser and Piller, 2004; Magyar et al., 1999.

* Corresponding author.
E-mail address: d.v.palcu@uu.nl (D.V. Palcu).

http://dx.doi.org/10.1016/j.gloplacha.2017.09.013
Received 11 February 2017; Received in revised form 29 August 2017; Accepted 20 September 2017
Available online 22 September 2017

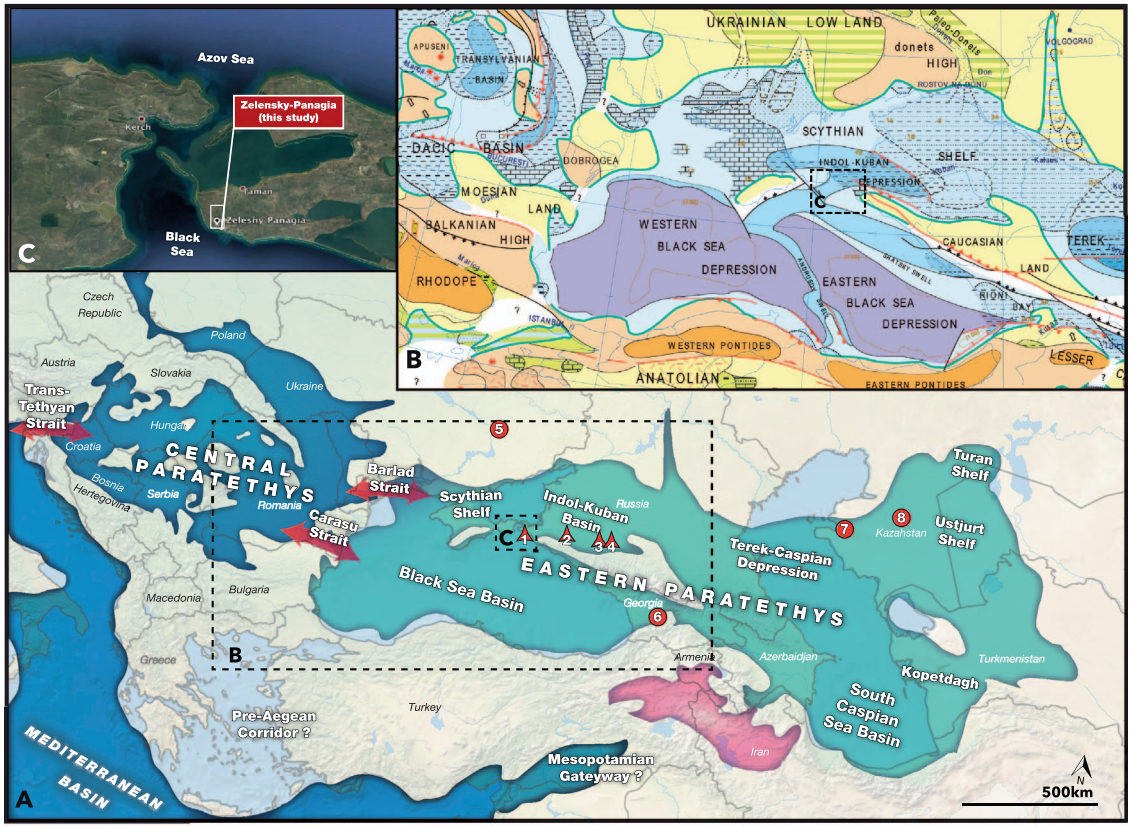

Fig. 1. (A) The Paratethys realm and its major sub-basins as suggested by the distribution of middle Miocene sediments. Marine gateways are figured as red arrows. Geographic position of sections where bio-magneto-stratigraphic studies were conducted (1.Zelensky, 2.CK12000, 3.Pshekha, 4.Belaya) and sections where biostratigraphy was performed (5.Konka River, 6.Naspere, 7.Ujratam, 8.Aschiktaypak); (B) Paleogeographic map for the mid-Konkian – upper Badenian (Kosovian) time (after Popov et al., 2004 map 6) and position of studied section. (C) Zoom on the study area. (For interpretation of the references to colour in this figure legend, the reader is referred to the web version of this article.)

A reliable time frame for the basinal Paratethyan successions is essential to unravel the geodynamic and climatic forcing factors of gateway restriction and to understand the mechanism of paleoenvironmental change. During the last decade, significant progress has been made to date the Central Paratethys successions by radiometric dating and magnetostratigraphy (e.g. Handler et al., 2006; Hohenegger et al., 2009; Vasiliev et al., 2010; De Leeuw et al., 2010, De Leeuw et al., 2013; Bukowski et al., 2010; Paulissen et al., 2011; Selmeczi et al., 2012; Śliwiński et al., 2012; Mandic et al., 2011; ter Borgh et al., 2013; Palcu et al., 2015), allowing correlations to the open ocean climate and sea level records. Radiometric dating indicated that the onset of the BSC in the Paratethys took place at 13.8 Ma and was primarily controlled by climatic changes and in particular by the Mi3 global cooling event which terminates the Middle Miocene Climatic Optimum (De Leeuw et al., 2010). Magnetostratigraphic dating of the BSEE indicated an age of 12.65 Ma which, in contrast, suggested a tectonic forcing affecting in particular the Barlad gateway to the Eastern Paratethys and increasing interbasinal connectivity (Palcu et al., 2015). Magneto-biostratigraphy in combination with radiometric dating showed that the transition to low salinity water conditions of the Pannonian stage was triggered by tectonic uplift of the Carpathians (ter Borgh et al., 2013). Although these Central Paratethyan events have been the subject of intense study, many key questions concerning the mechanisms of their onset, progression and termination remain unanswered especially because the temporal evolution of the Eastern Paratethys region is poorly constrained (e.g. Popov et al., 2006).

The Middle Miocene stratigraphic framework of the Eastern Paratethys is largely based on transgressive-regressive cycles and characteristic faunal assemblages reflecting changes in the hydrological regime of this semi-enclosed basin (Nevesskaya et al., 2005a; Popov et al., 2006). Radiometric and magnetostratigraphic age constraints for this region are notoriously lacking. The fragmentation and subsequent isolation of the Eastern Paratethys led to the development of biota that are characterized by recurrent endemism. These endemic faunal assemblages hamper straightforward correlations to the Geological Time Scale and led to the establishment of numerous regional stages (Tarkhanian, Chokrakian, Karaganian, Konkian and Volhynian), all with very limited age constraints (Fig. 2).

In this paper we establish a new chronological framework for the sedimentary successions of the Eastern Paratethys by applying integrated magneto-biostratigraphic dating techniques to the uppermost Chokrakian-Volhynian successions of the Zelensky-Panagia section (Fig. 1c). Zelensky-Panagia is located in the Taman Peninsula in Southern Russia and it represents a continuous outer shelf depositional facies in the northern part of the Euxinic Basin and can therefore be considered an archetype for Eastern Paratethys environmental change. Our new time frame allows a direct correlation of the Eastern Paratethys stratigraphy to the Central Paratethys successions and a better understanding of the mechanisms of paleoenvironmental change in both restricted basins. The results will be discussed in the context of gateway evolution and hydrological changes affecting the connectivity between the two Paratethys domains.

2. Geological and stratigraphic background

The epicontinental Paratethys Sea became progressively separated from the Mediterranean basin by tectonic uplift of the Alpine-Balkan-Pontides-Alborz-Kopetdagh orogenic belt since the early Oligocene (e.g. Rogl, 1999). During the Middle Miocene, Paratethys covered the area from the Vienna Basin in Austria to the Kopetdagh region in Turkmenistan (Popov et al., 2006). Paratethys was fragmented in smaller subbasins that were grouped in two systems: the Central European (Central

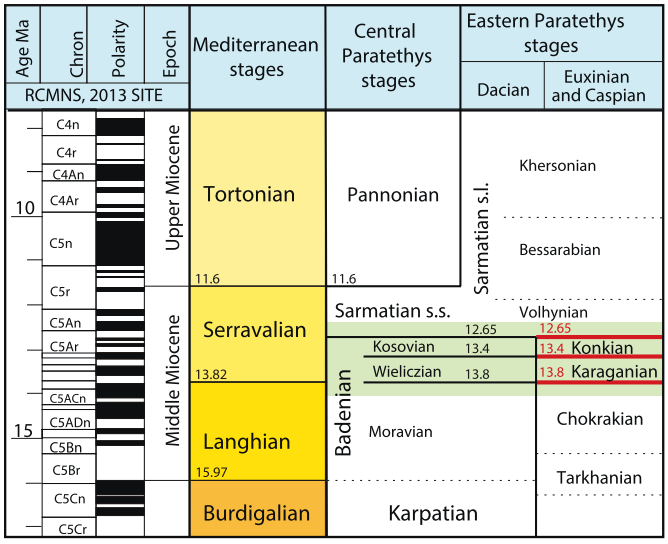

Fig. 2. Middle Miocene stratigraphy of the Mediterranean, Central Paratethys and Eastern Paratethys (Hilgen et al., 2012, updated by Palcu et al., 2015). The time interval of focus in this article in is marked in green. New ages documented by this study are marked in red. (For interpretation of the references to colour in this figure legend, the reader is referred to the web version of this article.)

Paratethys) and the Euxinian-Caspian (Eastern Paratethys). The latter basin system extended from northeast Bulgaria and the eastern slopes of the Dobrogea Mountains of Romania to the Ustjurt and Kopetdagh in Central Asia (Fig.1a). Shallow environments dominated the Scythian and Turanian shelfs; deep ones are preserved in the relict Western and Eastern Black Sea and South Caspian depression and in the Indol-Kubanian and Terek-Caspian foredeeps (Fig. 1a). Episodes of relative isolation or poor connectivity of these basins with the global ocean impedes straightforward correlations with the global stratigraphy and therefore, regional stratigraphic stages have been defined for both Central and Eastern Paratethys (e.g. Hilgen et al., 2012).

The Neogene stratigraphic scale of the Eastern Paratethys Middle Miocene was created 100–150 years ago by Barbot de Marny (1866) and Andrusov (1917). Stratigraphic horizons in this scale have later been upgraded to the rank of regional stages at the VI Congress RCMNS in 1975, (Proc. 6th Congress RCMNS, Vol. 2, 1976, p. 65, 66) at the same time as the Central Paratethys stratigraphic units (Fig.2). The stratotypes of the regional stages were proposed in relatively shallow basins where the stratigraphic successions are generally incomplete, but where the mollusk assemblages (the main stratigraphic group in Andrussov's time) were best developed. Although these stratotypes have been excellent for describing the assemblages corresponding to each of the regional stages, continuous sections and integration of new methods are required to better understand and date the paleoenvironmental and paleoecological changes in the region. Complete successions of Karaganian, Konkian and Volhynian sediments are, however, mainly found from deep settings. These provide less abundant mollusk assemblages, but do contain richer assemblages of planktonic and benthic foraminifera and calcareous nannoplankton. In this paper, we focus on determining the age constraints for the Middle Miocene Karaganian, Konkian and Volhynian stages of the Eastern Paratethys.

The Karaganian (Andrusov, 1917) is characterized by low faunal diversity, suggesting a more restricted connectivity regime than in the previous Chokrakian stage. Traditionally, it is correlated with the lower Serravallian and the middle part of the Badenian Stage of the neighboring Central Paratethys (Fig. 2), due to its position between the planktonic zones NN5 (in the mid-Tarkhanian) and NN6 (in the mid-Konkian) (Nevesskaya et al., 2005a). The Karaganian stratotype section is located in Uyratam, in the Mangyshlak Peninsula of Kazakhstan (Andrusov, 1917; Goncharova and Karaganian, 1975). Another key-section is present along the Belaya River in Ciscaucasia (Russia), where a rather complete succession of shallow facies is preserved (Nevesskaya et al., 2005b; Popov et al., 2016). The Zelensky-Panagia coastal section on the Taman Peninsula represents a deep water faciostratotype, significantly deeper than that of the stratotype Uyratam and Belaya River sections.

The Konkian (Michaylovskiy, 1909) contains deposits with marine mollusk associations in its shallow facies and characteristic foraminiferal assemblages, including planktonic forms in deeper facies. From the nannoplankton perspective it corresponds to the NN6-NN7 Zone (Nevesskaya et al., 2005a), corresponding to the Serravallian and to the upper Badenian (Kosovian) stage of Central Paratethys (Fig. 2). The Konkian stratotype section is located along the Konka River near Veselyanka Village in Ukraine and was originally described as "beds with *Venus konkensis*" (Sokolov, 1899). The section only comprises the upper Konkian "Veselyanka Beds", as the lower Konkian units are missing. The lack of a complete succession in the stratoype locality has led to various, often conflicting, views and interpretations on the volume and stratigraphic subdivision of the Konkian stage and especially on its lower boundary (see Vernigorova, 2009 for a review). In our work we follow the Konkian view sensu Merklin (1953), which comprises in stratigraphic order the Kartvelian (beds with abundant *Barnea* in shallow facies), the Sartaganian (beds with most diverse marine fauna) and the Veselyankian (beds with marine euryhaline fauna). In the relatively deep-water sections, beds with abundant *Barnea* sp. are absent, but the layers below the Sartaganian deposits comprise marine Konkian foraminifera (Vernigorova et al., 2006). Their species diversity makes it possible to define the initial development stage of the Konkian basin (Vernyhorova, 2015) or the Kartvelian substage (sensu Merklin, 1953). Complete sections, comprising all subunits of the Konkian regiostage, are situated on the Black Sea coast of Taman Peninsula (Vernigorova et al., 2006; Popov et al., 2016).

The Volhynian is the lowermost substage of the Sarmatian (sensu *lato*), which was proposed by N. Barbot de Marny, published by E. Suess, 1866 with reference to Barbot de Marny authorship. The (lecto) stratotype is the Ingulec River section near Dnepropetrovsk in Ukraine (Paramonova and Belokrys, 1972). Other sections with good, continuous exposure are found on the Black Sea coast of the Taman Peninsula.

The Sarmatian s.l. is subdivided into three regional substages: Volhynian, Bessarabian and Khersonian, mostly on the basis of mollusk and foraminifer assemblages. The Volhynian corresponds to the upper Serravalian, the Bessarabian and the Khersonian are correlated with the Tortonian (Nevesskaya et al., 2005a; Radionova et al., 2012). The Volhynian and lower part of the Bessarabian are correlated with the Sarmatian s.str. (sensu Suess, 1866) of the Central Paratethys. We refrain in our work to apply the term Sarmatian s.l. and we will use the substages Volhynian, Bessarabian and Khersonian for the Eastern Paratethys to avoid confusion in nomenclature.

The Black Sea coast outcrops of the Taman Peninsula (Fig. 3) compose an almost continuous succession from the upper Chokrakian to the Kimmerian, ranging from the Middle Miocene to Pliocene. They are exposed in a system of synclinal and anticlinal folds. The Late Miocene-Pliocene part of the succession was recently studied in high-resolution (Krijgsman et al., 2010; Vasiliev et al., 2011; Radionova et al., 2012; Rybkina et al., 2015; Stoica et al., 2016; Popov et al., 2016). Here, we focus our study on the core of the Zelensky-Panagia anticline, containing clays and marls of late Chokrakian – Karaganian – Konkian – Volhynian Age. These deposits consist of a monotonous sequence of clays, rhythmically interrupted by whitish marly intercalations (Fig. 3). The section was logged in detail, with the characteristic white concretion levels numbered upward in successive order (Fig. 4), and sampled for biostratigraphic and paleomagnetic purposes on the western flank of the anticline at geographical coordinates 45° 8′7.61″N/36°39′8.37″E.

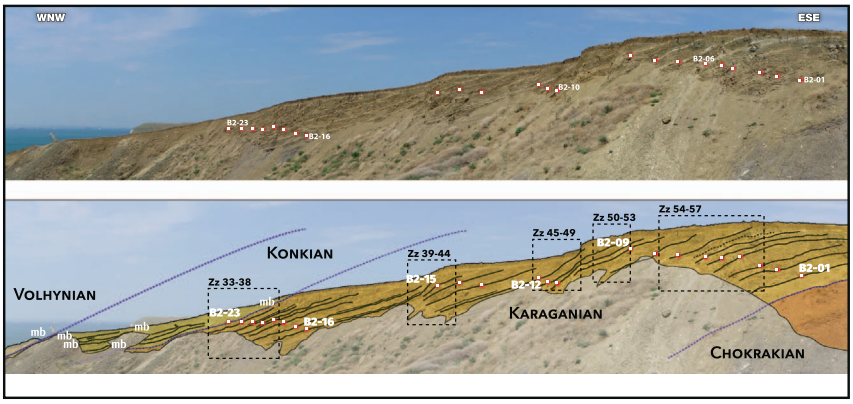

Fig. 3. Overview on the middle and lower part of the Zelensky-Panagia Section and an explanatory sketch with highlights on the sampling areas (marked in black) and the marker beds (represented in white) to emphasize the cyclic aspect of the section.

3. Biostratigraphy

Utilizing integrated stratigraphy we aim to provide age constraints on the Karaganian–Konkian–Volhynian stages of the Eastern Paratethys. Biostratigraphically we focus on the mollusk, foraminifera, and calcareous nannoplankton assemblages that can be used to identify and locate the stage boundaries and to provide supplementary information on the environmental changes in the basin. Macrofossils are scarce but the foraminifera and nannofossils are generally well preserved. The selection and determination of foraminifera was made from 250 g of rock sample that had previously washed through a 76 μm sieve (e.g. Vernigorova et al., 2006). To identify nannofossils, smear slides were prepared using standard procedures (e.g. Golovina et al., 2004) and examined under a Jena/Zeiss light microscope (cross and parallel nicols) at ×1200 magnification. Additionally key foraminifera and nannofossils were examined under SEM (scanning electron microscope) (Popov et al., 2016).

3.1. Mollusks

The relatively deep-water facies of the Middle Miocene deposits of the Taman Peninsula are not very favorable to provide abundant and rich associations of mollusks. Nevertheless, the few observed species are informative and show that all regional substages of the Middle Miocene are present in the sampled succession. The lowermost part of the section (units A and B1) contains specimens of *Lutetia* (*Davidaschvilia*) *intermedia* (Fig. 4), which imply an upper Chokrakian age (Goncharova in Golovina et al., 2004). The lower half of B2 is characterized by small and poorly preserved, difficult to determine, forms of *Lutetia* (*Davidaschvilia*) *intermedia* or *Zhgentiana gentilis* (Eichw.). Though poorly preserved, the fauna can be interpreted as corresponding to the Karaganian stage. In the upper part of B2, the presence of *Zhgentiana gentilis* (Eichw.) and *Zhgentia* cf. *grandis* (Andrus.) indicates a Karaganian age. Unit C does not contain any mollusks but the clays of unit D are marked in the lower part by occurrences of *Ervilia* and *Abra* and in the upper part by *Mytilaster volhynicus* (Eichw.), *Ervilia pusila trigonula* Sok., *Modiolus* sp.,? *Barnea* sp.,? *Abra* sp., *Timoclea konkensis* and *Alveinus nitidus*, the latter ones being characteristic for the Konkian stage. In unit G, approximately 4 m above marker bed E, *Abra alba scythica* (Sok.), rare *Musculus* sp. and *Mactra* sp. are found, which correspond to the Volhynian.

3.2. Foraminifera

The foraminifera from units A, B1 and B2 have previously been investigated (T. Pinchuk in Popov et al., 2009). Units A and B1 (Fig. 4) comprise members of the genera *Hyperammina*, *Saccammina*, species of the genera *Quinqueloculina*, *Sigmoilina*, *Spiroloculina* and *Discorbis tschokrakensis* Bogd, an association that corresponds to beds with *Florilus parvus* of the late Chokrakian (Bogdanovich, 1965). In unit B2, a poor association of *Saccammina*, *Nonion*, *Quinqueloculina* and *Discorbis* was found. It includes *D. urupensis* Krasch. and *D. kartvelicus* Krash., which are characteristic for the Karaganian (Pinchuk, 2006).

More diverse foraminiferal associations are present in the interval between units C and G (see also Vernigorova et al., 2006; Popov et al., 2016). Planktonic foraminifera are observed in almost all samples, but shells are generally rare and very small-sized. Benthic foraminiferal assemblages are more abundant and can be used to define the boundaries of the Konkian substages.

Unit C (Fig. 4) contains (albeit rare) *Quinqueloculina* ex gr. *consobrina* d'Orb., *Varidentella reussi sartaganica* Krash., *Nodobacullariella konkensis* Bogd., *Articulina vermicularis* Bogd., *Nonion tauricus* Krash., *Bolivina* sp., *Reussella spinulisa* (Reuss), *Cassidulina bulbiformis* Krash., *Discorbis kartvelicus* Krash., *D. supinus* Krash, an assemblage characteristic for the Konkian stage. Shells are generally small-sized and well preserved. The domination of *Cassidulina* and *Discorbis*, combined with the small number of the Konkian foraminifera, indicates correlations to the early development stage of the Konkian (Vernyhorova, 2015), the Kartvel beds (according to Krasheninnikov, 1959, Bogdanovich, 1965).

Unit D shows an assemblage marked by increased numbers of *Quinqueloculina angustissima* Bogd., *Q. guriana* O.Djan., *Q.* ex gr. *consobrina* d'Orb, *Varidentella reussi sartaganica* Krash., *Articulina cubanica* Bogd., *Nodobacullariella didkowskii* Bogd., *Bolivina* ex gr. *crenulata* Cush., *Discorbis kartvelicus* Krash., *Cassidulina bulbiformis* Krash., *Florilus boueanus* Orb., *Porosononion martkobi* (Bogd.), *P. subgranosus* (Egger) (Fig. 5). Species of *Quinqueloculina*, *Bolivina*, *Bulimina* genera are dominant but shells have small size, modified walls (thin, corroded) and are often poorly preserved. An abrupt change in species diversity is observed in the upper part of unit D, which comprises 55 species, belonging to 28 genera. The foraminiferal assemblages of unit D correlate to the Sartagan beds (according to Krasheninnikov, 1959, Vernigorova et al., 2006) or the Sartaganian substage (according to Dzhanelidze, 1970). The faunal assemblage of the Kartvelian and Sartaganian indicates marine environments and connectivity to the open ocean, because the species of the normal-marine genera: *Nodobacullariella*, *Articulina*, *Reussella*, *Cassidulina*, *Discorbis* (according to: Krasheninnikov, 1959, Bogdanovich, 1965; Vernigorova et al., 2006, Popov et al., 2016), dominate the assemblage.

In the terminal part of unit D, and in units E and F, a considerable reduction of species diversity is observed (Figs. 4, 5). Foraminiferal shells are generally rare and have small sizes. The presence of typical Konkian species *Quinqueloculina guriana*, *Varidentella reussi sartaganica*, *Discorbis supinus* together with the euryhaline species, *Elphidium horridum*, *Nonion bogdanowichi*, *Ammonia* ex gr. *beccarii* (also common in the Volhynian) are indicative for the final phase of the Konkian (by Bogdanovich, 1965, Vernyhorova, 2015), or to the Veselyanka beds (according to Krasheninnikov, 1959, Vernigorova et al., 2006) or the Veselyankian substage (by Dzhanelidze, 1970).

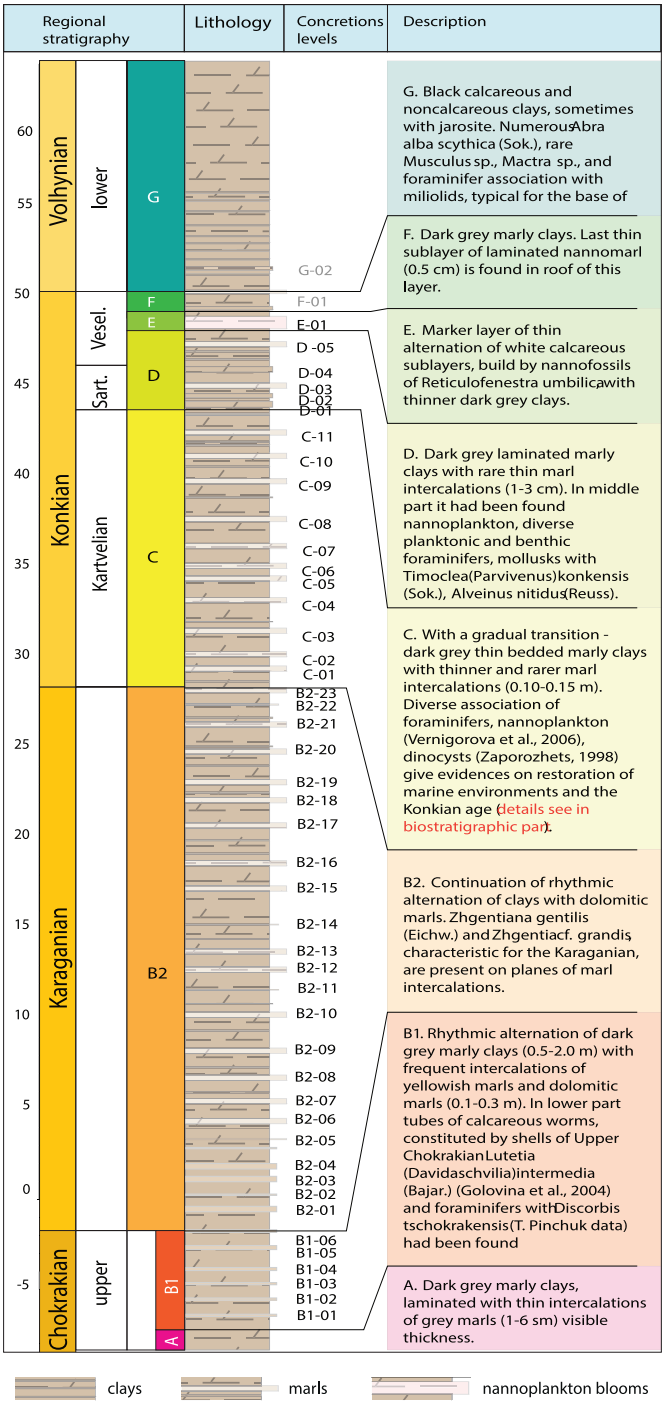

Fig. 4. Bio-litho-stratigraphic schematic description of the Zelensky-Panagia Section.

The lower half of Unit G (Fig. 5) has only a few poorly preserved foraminifera shells of *Porosononion* genus. However, the upper half of this Unit (not presented here) is characterized by relatively rich benthic foraminifera (25 species, according to Pinchuk in Popov et al., 2011), and *Miliolinella*, *Quinqueloculina*, *Articulina*, *Porosononion*, *Nonion*, *Elphidium* are constantly present (according to Pinchuk and Verhyhorova in Popov et al., 2016). Species of *Quinqueloculina* are prevailing in the clays, while species of *Elphidium* dominate the marls. The presence of *Quinqueloculina reussi reussi*, *Articulina sarmatica*, *Elphidium josephina* (d'Orb), indicates a correlation to the Volhynian (sensu Bogdanovich, 1965).

3.3. Calcareous nannoplankton

Units A, B1 and B2 do not contain nannofossils (Figs. 4, 5). The first manifestation of nannoplankton is noted at the base of unit C, where assemblages mainly consist of *Braarudosphaera bigelowii* (Gran & Braarud 1935) Deflandre, 1947, *Calcidiscus leptoporus* (Murray & Blackman 1898) Loeblich & Tappan, 1978, *Coccolithus pelagicus* (Wallich 1877) Schiller, 1930, *Cyclicargolithus floridanus* (Roth & Hay, in Hay et al., 1967) Bukry, 1971, *Pontosphaera multipora* (Kamptner, 1948 ex Deflandre, 1954) Roth, 1970, *Reticulofenestra pseudoumbilicus* (Gartner, 1967) Gartner, 1969, *Reticulofenestra* sp., *Thoracosphaera* sp. (Fig. 5). Unit D is marked by an increase in biodiversity. Its typical association is composed of *Cricolithus jonesi* Cohen, 1965, *Helicosphaera carteri* (Wallich 1877) Kamptner, 1954, *Helicosphaera* sp., *Rhabdosphaera pannonica* Baldi-Beke (1960), *Rhabdosphaera sicca* (Stradner, 1963), *Rhabdosphaera poculii* (Bona and Kernene, 1974) Muller, 1974, *Rhabdosphaera* sp., *Sphenolithus moriformis* (Bronnimann and Stradner, 1960) Bramlette and Wilcoxon, 1967. The white marly intercalations in this unit are characterized by monospecific *Reticulofenestra pseudoumbilicus*, abundant *Braarudosphaera bigelowii*, very rare *Rhabdosphaera poculii*, *Rhabdosphaera* sp. and a single specimen of *Discoaster* aff. *kugleri*. The assemblages of units C and D do not contain zonal markers but may correspond to the undivided interval of NN6 *Discoaster exilis* – NN 7 *Discoaster kugleri* (Martini, 1971). An increase of the bloom of *Reticulofenestra pseudoumbilicus* marks the upper part of unit D.

Unit E is characterized by the sedimentation of coccolithic laminated limestone, represented by monospecific *Reticulofenestra pseudoumbilicus*, while rare *Braarudosphaera bigelowii*, a single *Rhabdosphaera poculii* and very small *Syracosphaera* sp. are also present (Fig. 4). These coccolithic limestones reflect specific paleoenvironmental conditions, and probably relate to periods of stratification and high nutrient input. The latest bloom of *Reticulofenestra pseudoumbilicus* is observed at the top of unit F in a very thin (0.5 cm) sublayer of calcareous clays. It is worth mentioning that although not included in Fig. 5 because of their scarcity, most deposits of the unit F, contain very rare *Coccolithus pelagicus* (Wallich 1877) Schiller, 1930, *Cyclicargolithus floridanus* (Roth & Hay, in Hay et al., 1967) Bukry, 1971 and *Sphenolithus moriformis* (Bronnimann and Stradner, 1960) Bramlette and Wilcoxon, 1967 (Popov et al., 2016). Also, rare *Lacunolithus menneri* Lulejewa, 1989 is identified at the base of unit G but has not been pictured in Fig. 5 due to its scarcity.

3.4. Regional biostratigraphic framework

The mollusk and foraminiferal assemblages of the Zelensky-Panagia section both indicate that the Chokrakian-Karaganian boundary is located at the transition between Units B1 and B2 at level –2 m (Fig. 4). The Karaganian fossil assemblages indicate a decrease in salinity and are indicative of more restricted connectivity, probably implying isolation of the Eastern Paratethys basin from the open ocean. The first occurrence of calcareous nannofossils and planktonic and benthic foraminifera typical for the Konkian stage is found at the base of Unit C. This level determines the Karaganian-Konkian boundary (at 27.9 m), which reflects a transition to marine environments and re-connectivity to the open ocean.

The Konkian deposits comprise a continuous succession and can be subdivided in three substages according to the foraminifera and calcareous nannoplankton assemblages. The Kartvelian substage is characterized by the first appearance of nannoplankton, the presence of the planktonic foraminifer *Globigerina* genus and the marine benthic foraminifer genera: *Discorbis*, *Cassidulina*, *Articulina* and scarce *Nodobaculariella*, *Reussella*. In the Kartvelian part of the section no mollusks are found.

The Sartaganian substage contains more diverse nannoplankton and foraminiferal assemblages. Both planktonic and benthic groups show quantitative and qualitative variations in composition, most likely

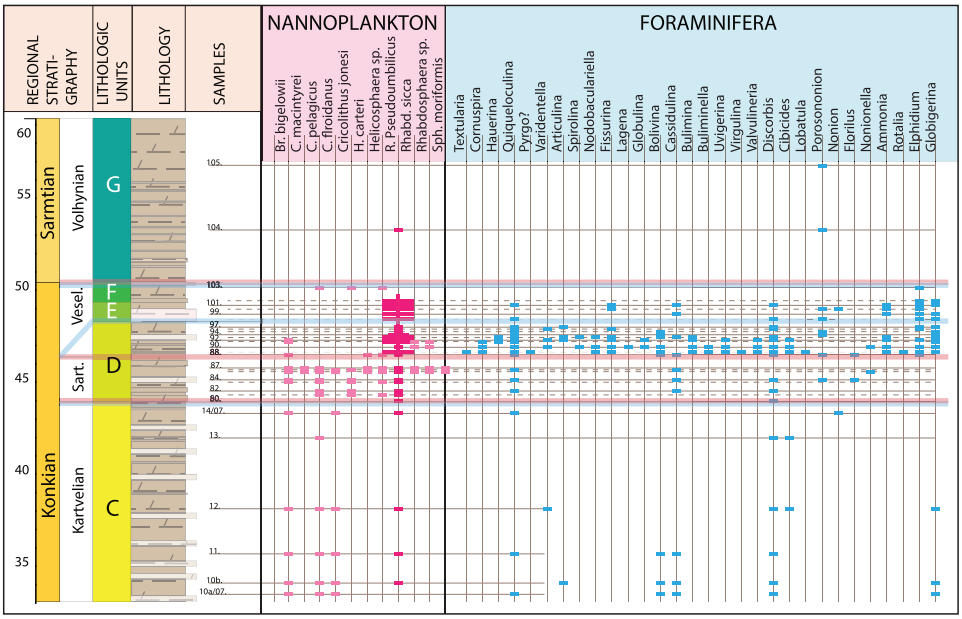

Fig. 5. Stratigraphic distribution of nannoplankton and foraminifera species in Zelensky-Panagia Section. Note the two interpretations on the Sartaganian - Veselyankian boundary, following the information on the nannoplankton and foraminifera distribution. The large occurrences of *R. pseudoumbilicus* are repetitive blooms.

reflecting pulsating marine influxes (fluctuations of salinity, temperature and nutrient input), indicative for an unstable marine environment. The main environmental changes took place during the upper part of the Sartaganian, where levels of monospecific coccoliths reflect a transformation towards non-marine conditions in the surface waters of the basin. At the same time, the benthic microfauna shows changes towards increasing marine assemblages, indicating more stable marine environments at the deeper settings. Various other fossils have been found in the Sartaganian part of the section (bones of fish and seals, imprints of insects, fragments of bryozoans, ostracods, plant seeds, etc.). The ostracod assemblage comprises *Hemicytheria* ex gr. *cancellata* (Lienenklaus), *Cytherura fragilis* (Stancheva), *Aurila* cf. *notata* (Reuss), *Loxoconcha biblicata* Schneider, *Cytherura lamellosa* Scher. et Tschab., *Leptocythere distenta* Schneider, *Xestoleberis* (*Xestoleberis*) *lutrae* Schneider, *Cyprideis torosa* Jones (V.A. Kovalenko in Vernigorova et al., 2006). The Veselyankian substage comprises poor benthic foraminiferal assemblages and shows various blooms of *Reticulofenestra pseudoumbilicus*, reflected by the deposition of coccolithic limestones. It should be noted that a small offset in the location of the boundary (see Fig. 5) between the main and the final phases (the Sartaganian and Veselyankian) exists between the interpretations of the foraminifer and nannoplankton data (Vernyhorova et al., 2006). The Konkian-Volhynian boundary is determined by the onset of the typical Volhynian assemblages at the unit G, after the final bloom of *Reticulofenestra pseudoumbilicus* at top of unit F (at level 50.35 m).

4. Magnetostratigraphy

Magnetostratigraphy can provide ages to rock successions if the established polarity pattern of the studied sections can be correlated to reversal pattern of the Geomagnetic Polarity Time Scale (e.g. Langereis et al., 2010). Magnetostratigraphy has earlier been proven to be very useful, especially in Central Paratethys sediments for a variety of magnetic carriers (Vasiliev et al., 2010; Paulissen et al., 2011; De Leeuw et al., 2013; Ter Borgh et al. 2013).

The Zelensky-Panagia section was sampled at meter-scale resolution with a hand-held electric drill using water as a coolant. Paleomagnetic cores were collected from a total of 57 levels. The orientation of the paleomagnetic cores and the corresponding bedding planes were obtained using a magnetic compass, previously corrected for the local magnetic declination.

In the field, the magnetic susceptibility was measured with a SM30 magnetic susceptibility meter. The SM30 has an 8 kHz LC oscillator with a large size pick-up coil as a sensor that ensures a good penetration depth: 90% of its signal penetrates the first 20 mm of the measured level. The magnetic susceptibility was measured on 216 levels, corresponding to a resolution of 25–30 cm. The susceptibility record may indicate changes in the nature of the carriers and could highlight changes in the basin chemistry. We especially use this method to verify if there is a similar change in the magnetic properties of the Eastern Paratethys, as observed across the Badenian-Volhynian boundary in the Tisa section of the Central Paratethys (Palcu et al., 2015).

In the paleomagnetic laboratory of Fort Hoofddijk, rock-magnetic measurements were conducted to understand the nature of the magnetic carriers and to validate the magnetic susceptibility measurements from the field. These tests include measurements of magnetic susceptibility and thermomagnetic runs in air. The magnetic susceptibility in the lab was measured at room temperature for all cores, cut to a standardized length of 1 in., on a Kappabridge KLY-1. Thermomagnetic runs were measured in air on a modified horizontal translation type Curie balance with a sensitivity of approximately $5\ \text{Å} \sim 10-9\ \text{Am}^2$ (Mullender et al., 1993). Approximately 60 mg of powdered sample (put into a quartz glass sample holder and held in place by quartz wool) were heated and cooled at rates of 10 °C/min.

Afterwards, thermal and alternating field demagnetiszation techniques were applied to isolate the characteristic remanent magnetization (ChRM). The Natural Remanent Magnetization (NRM) was thermally demagnetized and measured using a 2G Enterprises DC Squid cryogenic magnetometer (noise level of $3 * 10–12\ \text{Am}^2$). The heating was obtained with the help of a laboratory-built, magnetically shielded furnace, with a residual field less than 10nT. The thermal steps are based on the observations on the behavior during the thermomagnetic runs. For the samples from Zelensky-Panagia, relatively small temperature steps of 10–30 °C were applied in the 100–360 °C range because of the rapid thermal decay and the occurrence of additional secondary magnetic carriers after 400 °C. Alternating field demagnetization was performed, with small field increments, up to a maximum of 100mT. An in-house built automated sample handler, attached to a horizontal 2G Enterprises DC SQUID cryogenic magnetometer was used for these measurements.

4.1. Rock magnetism

The magnetic susceptibility fluctuates significantly over the

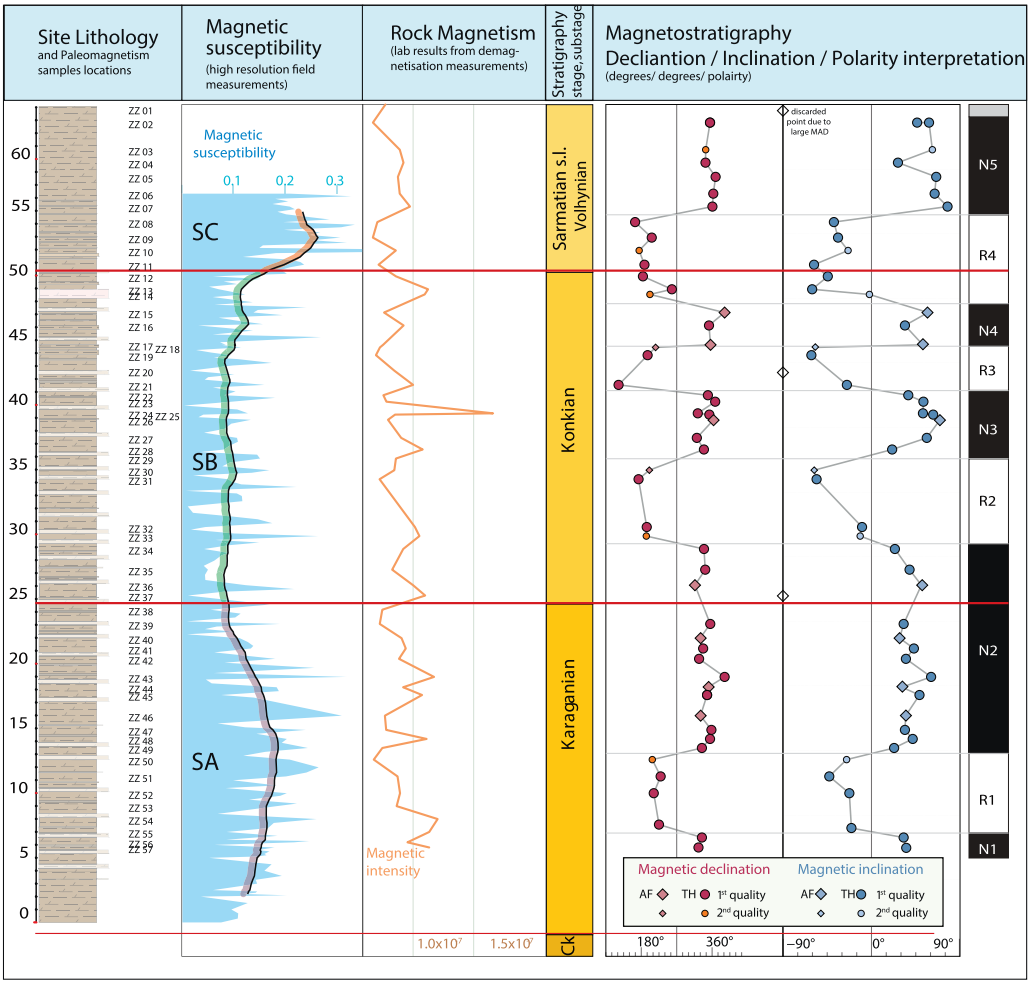

Fig. 6. Schematic lithological column, polarity zones, magnetic intensity and magnetic susceptibility for the Zelensky-Panagia section. Four reversed polarity intervals (R1, R2, R3, R4) and five normal ones (N1, N2, N3, N4, N5) have been identified. The positions of the stage boundaries are marked with red lines. The different trends of the magnetic susceptibility (blue): slow rise and fall in the SA zone - Karaganian, fluctuating in the SB zone - Konkian and abruptly increasing in the SC zone - Volhynian. (For interpretation of the references to colour in this figure legend, the reader is referred to the web version of this article.)

Zelensky-Panagia section, by more than two orders of magnitude (between 0.0029 and 0.438). Three zones (Fig. 6) can be distinguished based on the susceptibility trends. In the Karaganian part of the section (SA), the susceptibility first slowly increases up to 0.221E-05 m^3/kg at the 16 m and then decreases back towards initial levels at 24.75 m. The Konkian part of the section (SB) is characterized by remarkably steady values of around 0.068E-05 m^3/kg. The Volhynian part of the section (SC) shows a significant increase in the average magnetic susceptibility (0.187E-05 m^3/kg equal to an increase of 275% compared to the average value of the Konkian) with the maximum peaks of 0.438E-05 m^3/kg. The magnetic susceptibility measured in the lab on the magnetostratigraphic samples, ranges between 6.79E-08 m^3/kg and 1.5E-07 m^3/kg throughout the section and is fairly constant. No big fluctuations are visible in the lower and middle part of the section but a significant increase is observed in the Volhynian part of the section, in the interval above 50.35 m.

The thermomagnetic runs show significant variations that correlate with the stratigraphy. Samples corresponding to the Konkian and Volhynian stages show the alteration of an iron sulfide (pyrite) that above ~400 °C turns to a magnetic phase (magnetite) and finally above 580–600 °C, to hematite (Fig. 7a). This alteration appears not to be present in the samples corresponding to the Karaganian stage (Fig. 7a).

The majority of the Konkian and Volhynian samples show a reversible decrease (Fig. 7a), characteristic for magnetite. The Karaganian samples show a different behavior with increasing temperature up to ~410 °C: the decrease in magnetization is irreversible (Fig. 7b highlight), characteristic for greigite.

4.2. Magnetic polarity pattern

The NRM intensity ranges between 20 ∗ 10–6 A/m and 71.000 ∗ 10–4 A/m (Fig. 6). Several characteristic thermal demagnetization diagrams, of mostly marls and clays, are depicted in Fig. 7b. We identified the ChRM by analyzing the decay-curves and vector endpoint diagrams (Zijderveld, 1967). During both the progressive thermal demagnetization and the progressive alternating fields demagnetization, two magnetic components can be recognized. A very weak, low-temperature, viscous overprint is generally removed at 120 °C (Fig. 7b). A second, higher-temperature, component is demagnetized at temperatures between 120 °C and 300 °C. This component is of dual polarity and is interpreted as the ChRM. The ChRM directions were defined by at least four consecutive temperature steps and calculated with the use of principal component analysis (Kirschvink, 1980).

We use the maximum angular deviation (MAD) of the calculated directions to separate the results into three qualitative groups. The 1st quality (MAD = 0–5) and 2nd quality results (MAD = 5–10) have been used for plotting the polarity pattern (Fig. 6). The 3rd quality results (MAD > 15) have been discarded from the polarity pattern (Fig. 6).

The ChRM directions, magnetic intensity and magnetic susceptibility have been plotted against stratigraphic levels (Fig. 6). The polarity pattern of the Zelensky-Panagia section comprises nine different polarity intervals, four of reverse (R1–4) and five of normal (N1–5) polarity.

5. A magnetostratigraphic time frame for the Eastern Paratethys

We aim to obtain a robust time frame for the Karaganian, Konkian

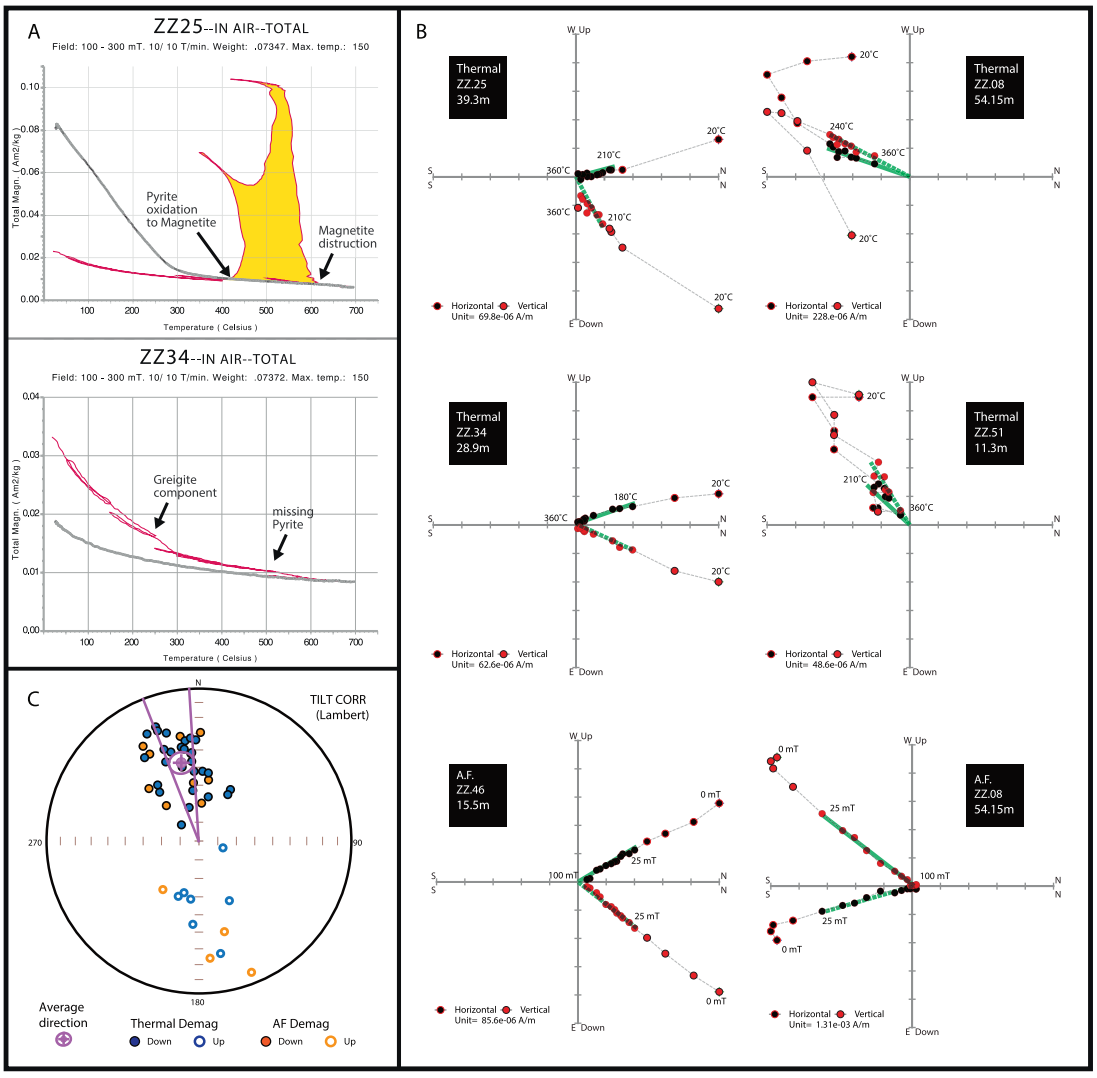

Fig. 7. (A) Thermo-magnetic runs for selected samples. Heating and cooling was performed with rates of 10 °C/min. Cycling field varied between 100 and 300 mT. Sample ZZ34, characteristic for the Karaganian samples, has a decay curve characteristic for a mix of greigite and magnetite, while missing pyrite. Sample ZZ25, characteristic for the Konkian and Volhynian samples, has a decay curve that corresponds to a magnetite signature and shows the intense oxidation of pyrite in magnetite above 415 °C. (B) Representative examples of Zijderveld demagnetization diagrams after tilt correction. Sample code and stratigraphic level are specified in the upper corner. Black (red) circles represent the projection on the horizontal (vertical) plane. The numbers represent the subsequent temperature demagnetization steps in degrees Celsius. The bold temperature values represent intervals used for calculating the ChRM component, which is marked by the green line. (C) Stereoplot of magnetic directions shows antipodal distribution of normal and reversed polarities. (For interpretation of the references to colour in this figure legend, the reader is referred to the web version of this article.)

and Volhynian deposits of the Eastern Paratethys by correlating the observed polarity pattern of the Zelensky-Panagia section to the astronomically dated polarity column of the most recent geomagnetic polarity time scale (GPTS) (Hilgen et al., 2012) (Figs. 8, 9). Biostratigraphic constraints restrict the Karaganian and Konkian part of the succession to the Serravallian and (upper) Badenian (Fig. 2), while the base of the Volhynian was recently dated at 12.65 Ma in the Carpathian foredeep of Romania (Palcu et al., 2015). This indicates that the age of the section is roughly limited to the time interval between 14 and 12 Ma, an interval with multiple magnetic reversals and a characteristic polarity pattern (Fig. 8).

Starting our correlation from the base of the section (marked by a red dotted square in Fig. 8), we notice that the Karaganian part is marked by a relatively short (6 m) reversed polarity interval R1, followed by a much longer (16 m) normal polarity interval N2 (Fig. 6). The 14–12 Ma time interval of the GPTS only shows two R-N chron pairs that have a normal chron that is longer than the preceding reversed chron: C5ACr/C5ACn and C5ABr/C5ABn.

The Konkian polarity pattern consists of two successive normal intervals (N3 and N4), of approximately similar length as reversed intervals (R2 and R3). Correlating R2/N3 (6 m/5 m) with C5AAr/C5AAn (180 kyr/151 kyr) seems straightforward, and fits much better than the correlation to C5ABr/C5ABn (245 kyr/131 kyr), suggesting that the younger correlation, N2 to C5ABn, is more sound. The polarity pattern straddling R3, N4, R4 remains problematic and cannot be directly correlated to the GPTS. However, we can use the top part of the polarity pattern (N5, R4, N4 – marked with a blue dotted square in Fig. 8) as another time constraint. The relatively long N5, followed by a long reverse R4 and a short normal N4 match, the pattern of chrons C5An.2n, C5.Ar.1r and C5.Ar.1n. The Konkian/Volhynian boundary is located in the lower part of reversed interval R4 that would correspond to chron C5Ar.1r. Both the chron and the position in the lower part of the chron are in good agreement with the magnetostratigraphic results from the Tisa section in Romania where the basal Volhynian is also correlated to the lower part of reversed chron C5Ar.1r (Palcu et al., 2015). The normal polarity interval N5 in the Volhynian then correlates to C5An.2n, which dates the top of our section at 12.3 Ma (Fig. 8). If we follow these constraints it is clear that our Konkian pattern with two

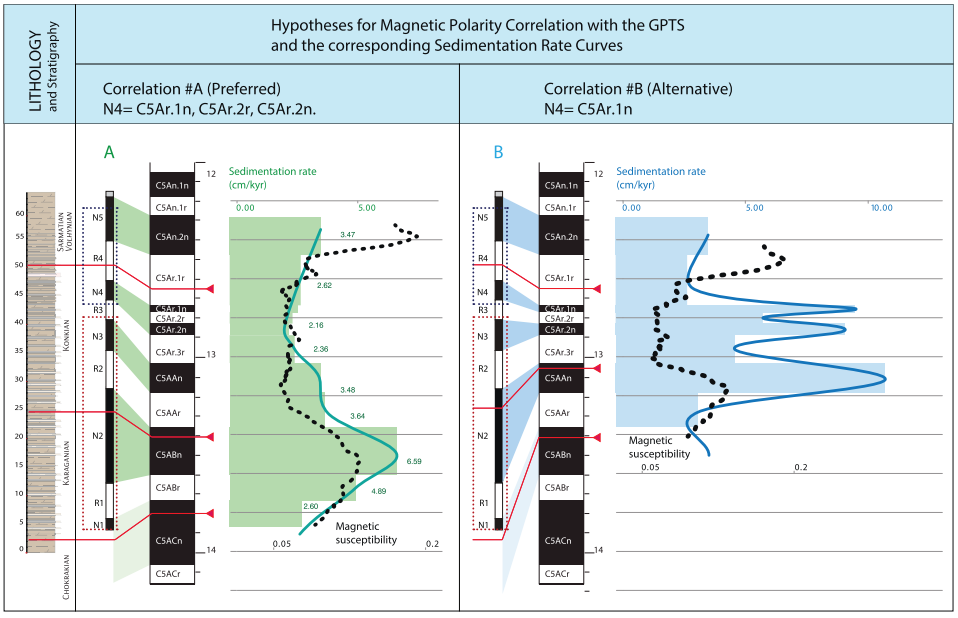

Fig. 8. Age model scenarios for the Zelensky-Panagia section: Preferred correlation (A) 13.8–12.4 Ma has a sedimentation rate that follows the magnetic susceptibility trend except for the uppermost part of the section, after the Ko/Vh boundary where the change in magnetic susceptibility is explained by a change in environment; (B) 13.4–12.4 Ma, shows large variations of sedimentation rates between the normal and reverse polarity intervals and does not correlate with the magnetic susceptibility trends.

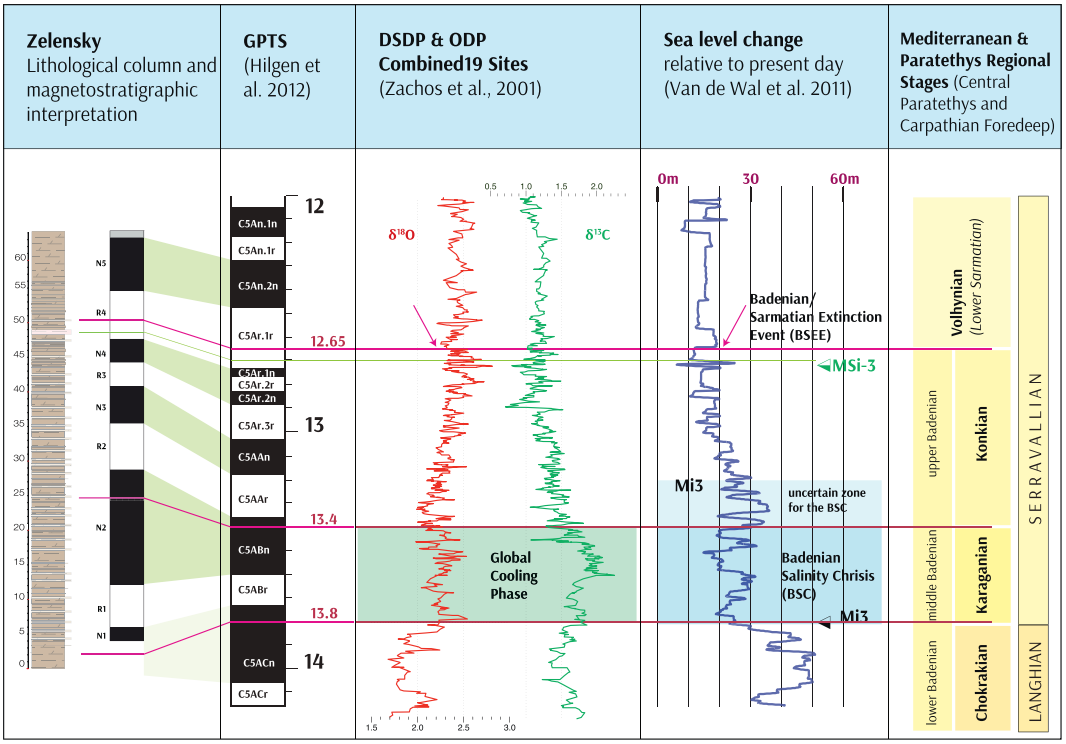

Fig. 9. Correlation of the polarity sequence of the Zelensky-Panagia section with the GPTS, the global oxygen & carbon isotope records and the sea-level fluctuations. The green bands correlate the polarity pattern of the section with the GPTS in the relevant time interval. The Karaganian corresponds to the Badenian Salinity crisis in Central Paratethys and the Ko/Vh boundary correlates to the BSEE. (For interpretation of the references to colour in this figure legend, the reader is referred to the web version of this article.)

normal intervals (N3, N4) does not match the three remaining normal chrons in the GPTS.

We have not seen any evidence for an unconformity in the succession, and all previous biostratigraphic studies indicate that the Zelensky-Panagia section is continuous (Golovina et al., 2004; Popov et al., 2009). Consequently, we conclude that it is more likely that our magnetostratigraphic pattern is incomplete for that interval. The most logical fit to the GPTS can be made if we assume that we have missed either subchron C5Ar.2r or C5Ar.1n in the interval straddling N4 (Fig. 8A). C5Ar.2r has a duration of 59 kyr in the GPTS, C5Ar.1n only 30 kyr, while our sampling resolution (57 samples/1.6 Myr) corresponds to an average of 1 sample/30 kyr. Hence, both subchrons should have been intercepted by one or two samples only, and it is thus not unlikely that one of them has been missed. If we correlate R3/N4/R4 (3 m/3 m/6 m) to the interval C5Ar.3r/C5Ar2n-C5Ar1n/C5Ar.1r (145 kyr/152 kyr/261 kyr) we obtain a very good fit. The sediment accumulation rates resulting from this correlation indicate gradual changes that seem to be in agreement with the lithological variations in the section. The Karaganian stage has significantly higher sedimentation rates than the Konkian, which positively correlates to the higher magnetic susceptibility in that interval (Fig. 8A). Variations in susceptibility may be related to changes in the ratio between clastic

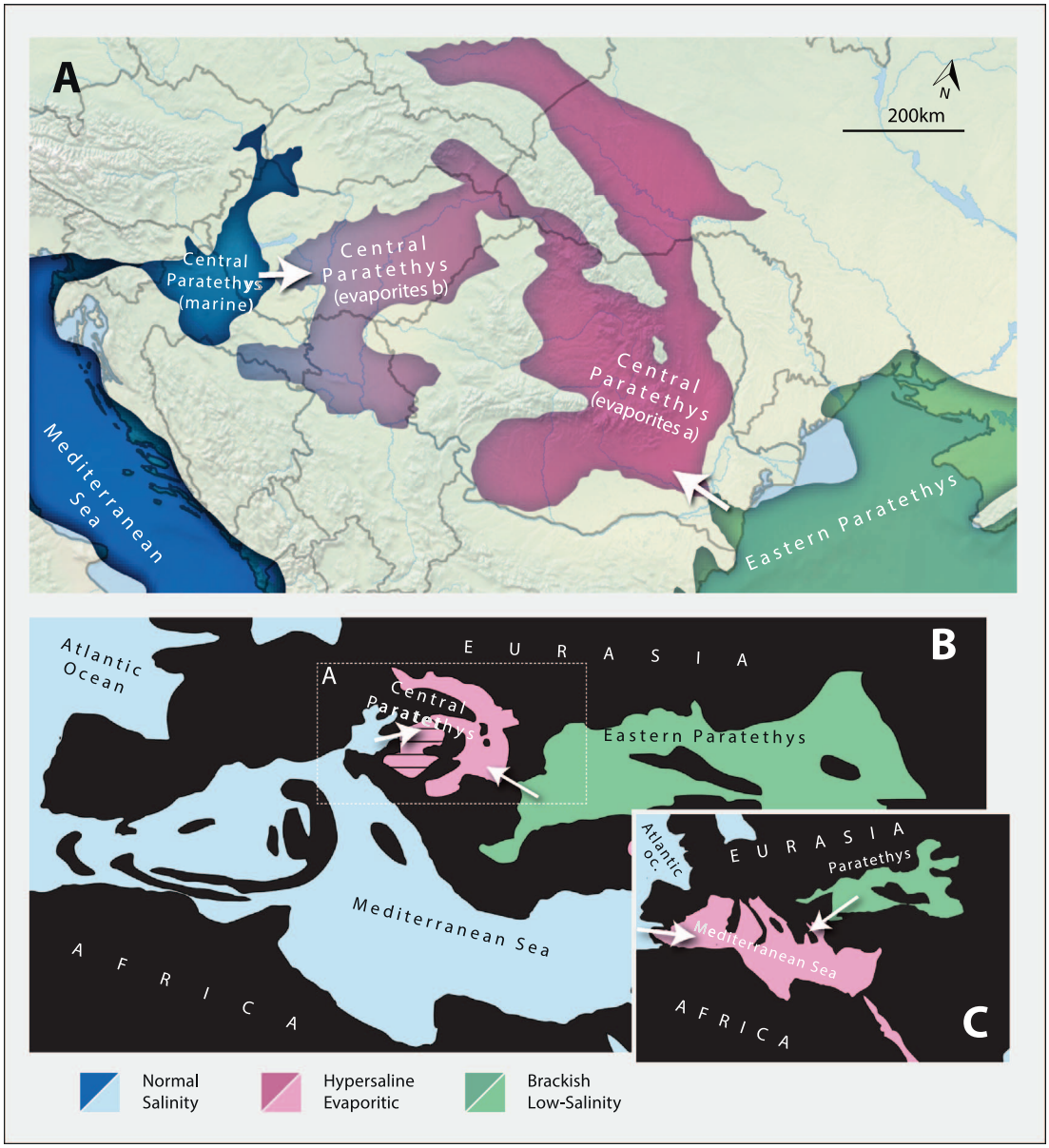

Fig. 10. (A) Paleogeographic configuration during the Badenian Salinity Crisis (BSC); (B) The evaporite basins of the Central Paratethys are located at the interference between low-salinity water flowing westwards through the Carasu/Barlad Strait from the Eastern Paratethys and marine water flowing eastwards through Trans-Tethyan corridor, in a context of restricted gateways. (C) This setting is strikingly similar with the flow configuration in the Mediterranean during the Messinian Salinity Crisis; 5.97–5.33 Ma.

sediments versus the biogenic and the chemical sediments, which are commonly related to environmental change (e.g. Oldfield, 2012; Thompson and Oldfield, 1986).

An alternative correlation can be made by starting from the top of the section, using the same constraints as before and correlating N5 and R4 to C5An.2n and C5Ar.1r, respectively. Downward correlation presents a reasonable fit by correlating N4, N3 and N2 to C5Ar.1n, C5Ar.2n and C5AAn (Fig. 8B). An irrational result of this correlation is that the accumulation rate in all normal intervals would be more than double the rate in the reversed intervals, a scenario that we consider highly unlikely.

In conclusion, we favor option A (Fig. 8A) as the best fit correlation of the Zelensky-Panagia polarity pattern to the GPTS. The subsequent magnetostratigraphic age constraints are the first for the Euxinic basin, and allow the construction of a revised time frame for the Middle Miocene stages of the Eastern Paratethys. Our preferred correlation indicates that the Chokrakian/Karaganian boundary is located in the upper part of C5ACn at an age of ~13.8 Ma (extrapolating ~7 m downwards following the sedimentation rate trend), closely corresponding to the Langhian/Serravallian boundary. The Karaganian/Konkian boundary is determined in the upper part of C5ABn at an age of 13.4 Ma and the Konkian/Volhynian boundary is dated in the lower part of C5Ar.1r at an age of 12.65 Ma (Fig. 9).

6. The influence of Paratethys gateway evolution on paleoenvironmental change

Our new results provide a more comprehensive picture on the paleogeographic changes that occurred in the middle Miocene of Central Europe, and shows that the operability of the Paratethys gateway is a key to understand the paleoenvironmental changes in the region. The latest Langhian interval is marked by restricted marine environments (Chokrakian) in the Eastern Paratethys and by open marine conditions (Lower Badenian) in the Central Paratethys. The presence of marine fauna in the Eastern Paratethys indicates that connectivity with the open ocean must have persisted in Chokrakian times, but that the

marine gateway with the Central Paratethys must have been limited in size, depth and width to prevent a full exchange between the two Paratethyan seas. During the early Serravallian, this gateway stopped functioning as a marine water source for Eastern Paratethys, which turned into a sea-lake during the Karaganian. The marine gateway that connected the Central Paratethys to the Mediterranean became restricted as well, culminating in hypersaline conditions and evaporite deposition in Central Paratethys during the Badenian Salinity Crisis. The BSC was ended by a marine incursion through the gateway(s) to Mediterranean that re-established open marine conditions in the Central Paratethys (Upper Badenian), which episodically influenced the Eastern Paratethys during the Konkian. The gateway between the Eastern Paratethys and Central Paratethys must have been limited in size again during the Konkian, and reached a new equilibrium phase in the early Sarmatian (Volhynian) when it became big enough to cause exchange between the Eastern and Central Paratethys seas, establishing rather uniform environments on both sides of the sill.

6.1. The Karaganian – expression and trigger of the Badenian salinity crisis?

The Chokrakian/Karaganian boundary corresponds to a significant change in Eastern Paratethyan mollusk, foraminifer, and nannoplankton faunas, all demonstrating that the marine species of the Chokrakian are replaced by species indicative of specific, semi-marine, conditions with unstable salinity of the Karaganian. Paleogeographically, the transition is interpreted as a change from a semi-closed Chokrakian sea towards a more restricted and fresher water sea-lake during the Karaganian (Peryt et al., 2004), indicating that Eastern Paratethys became isolated from the open ocean. In the Zelensky-Panagia section, the C/K boundary is marked by a lithological transition from dark grey marly clays of the Chokrakian towards rhythmic alternations of brown clays and white marly concretions of the Karaganian. The boundary level is placed at –2 m and corresponds, by extrapolation, to the upper part of chron C5ACn. Interpolation of sedimentation rates dates the boundary at an age of 13.8 Ma.

Correlation to the global climate and sea level curves indicates that the onset of the Karaganian closely correlates to the Mi3b cooling shift (Holbourn et al., 2013), suggesting a causal relationship (Fig. 9). This cooling step corresponds to the Langhian/Serravallian boundary (Hilgen et al., 2009) and is dated at 13.82 ± 0.03 Ma in the Mediterranean (Abels et al., 2005). It terminated the relatively warm climatic conditions of the Middle Miocene, as expressed in many isotope records worldwide (e.g., Holbourn et al., 2005, 2013). In Chokrakian times, the Eastern Paratethys was most likely connected to the Carpathian foredeep region in the west through the small and shallow "Carasu Strait" in the southern Dobrogea region of Romania (Fig. 10). The strait was identified in the area of the Carasu stream and contains shallow marine deposits with mostly Chokrakian fauna in the eastern (Chiriac, 1970) and (time-equivalent) Badenian fauna in the western part (Gradinaru, 2015). In the central part of the Carasu strait, the Badenian fauna reaches a maximum of ~35% of the total fauna but lacks its stenohaline elements such as corals, echinoderms and brachiopods (Chiriac, 1970). The Mi3b event is estimated to have caused a 40–50 m drop in global ocean level (John et al., 2011), which could have easily closed the Carasu Strait and isolated Eastern Paratethys from the global ocean.

The Mi3b sea level drop is also inferred to have affected the environmental conditions in the Central Paratethys. Oxygen isotope values of foraminifera show a major cooling trend in the lower Badenian just before the BSC evaporites (Bicchi et al., 2003). Moreover, warm-water planktonic foraminiferal assemblages are shown to be replaced by cool-water populations (Gonera et al., 2000), while a decline in thermophilous mollusk taxa is also observed (Harzhauser and Piller, 2007). $^{40}Ar/^{39}Ar$ dating of volcanic tuffs from directly below the Badenian salts shows that the onset of the BSC is dated at 13.81 ± 0.08 Ma, suggesting a causal relationship with the Mi3b cooling event as well (De Leeuw et al., 2010). The corresponding sea-level drop is considered to have restricted the water exchange through the marine gateways connecting Central Europe with the Mediterranean, resulting in hypersaline conditions in several Central Paratethys basins.

Our results indicate that the paleogeographic and hydrological configuration of the Central Paratethys during the BSC is slightly more complicated than previously envisaged (e.g. Rögl, 1998; De Leeuw et al., 2010, Báldi et al., 2015, Szuromi-Korecz and Selmeczi, 2015, Báldi et al., 2017). The peripheral basins of Central Europe that experienced hypersaline conditions and salt deposition are not only influenced by changes in the Mediterranean gateway, but also may have experienced different hydrological fluxes from the Eastern Paratethys. The Karaganian successions are commonly found transgressive on the marginal regions of the Black Sea basin (Popov et al., 2006), indicating that the hydrological budget of the Eastern Paratethys was positive during this time interval. The Carasu Strait has thus persisted during Karaganian times, connecting Eastern Paratethys (in a process of freshening) with the hypersaline Central Paratethys. The lack of hypersaline influences in Eastern Paratethys points to a unidirectional flow of low-salinity water into the basins of the Central Paratethys from East to West.

BSC salt and gypsum formation is following the same East-West trend: evaporites are more developed close to the gateway region - Carpathian foredeep and Transylvanian Basin, less developed in the middle part of Central Paratethys – Slovak and Pannonian basin and absent in the areas furthest from the gateway – Vienna and Styrian basins. This distribution points towards a causal link between the inflow of low-salinity water from Eastern Paratethys and the evaporite formation during the BSC.

At first sight it seems rather counterintuitive that inflow of low-salinity water could play a role in the formation of evaporites in silled basins. However, also in case of the Messinian Salinity Crisis of the Mediterranean it has become clear that a positive brackish water influx from Paratethys may have played a significant role in the formation of gypsum and salt (Krijgsman et al., 2010; Roveri et al., 2014). Traditionally, gypsum formation is considered to result from enhanced (seasonal) drought during precession maxima (Krijgsman et al., 2001), but recently it has been shown from gypsum hydration water and the salinity of fluid inclusions that influx of freshwater was a major component during gypsum formation (Dela Pierre et al., 2015; Natalicchio et al., 2014; Evans et al., 2015). The paleogeographic configuration of the BSC and MSC are very similar, with the evaporite basins in intermediate position between the open ocean and the restricted brackish water domain of the Eastern Paratethys (Fig. 10B). Global climate models showed that the hydrological budget of the Eastern Paratethys was also positive during the MSC, providing continuous low-salinity water flow to the Mediterranean (De la Vara et al., 2016; Marzocchi et al., 2016). Low-salinity water inflow from the Eastern Paratethys may have contributed to increased stratification in the evaporite basin, by creating a brackish water surface unit on top of hypersaline waters, thereby effectively preventing deep water mixing and increasing brine formation by blocking deep overflow towards the open marine basin (e.g. Marzocchi et al., 2016).

6.2. The Konkian: episodic connections between Eastern and Central Paratethys - the opening of a new strait

The Karaganian/Konkian transition (beginning of Kartvelian) is marked by the first marine influxes, which ended the semi-isolated position of the Karaganian sea-lake in the Eastern Paratethys. The Konkian comprises several faunal elements (nannoplankton, foraminifera, mollusks) that are assumed to come from the Central Paratethys (Kosovian), indicating that two-way connectivity must have been re-established through the Paratethys gateway (Fig. 10). Marine

faunal assemblages of the Zelensky-Panagia section are much more diverse in the middle (Sartaganian) part of the Konkian showing that the marine gateway functioned most effectively during that time period (Fig. 4). The Karaganian/Konkian boundary, located at 44 m, is positioned at the upper part of C5ABn and is dated at ~13.4 Ma.

Correlation to the global climate and sea level curves shows that the boundary does not correspond to any major change in climate or global sea level (Fig. 8). Consequently, we infer that geodynamic changes in the gateway regions were responsible for the marine ingression. The lack of evidence for Konkian fauna in the Carasu Strait hints at the development of a new gateway between Central and Eastern Paratethys. Fossil distribution patterns in the upper Badenian and Konkian point towards the initiation of the Barlad Strait, north of Dobrogea through present-day Ukraine and Moldova (Studencka et al., 1998; Popov et al., 2006). During the Konkian, the Barlad Strait was probably still in an early opening stage, characterized by intermittent and poor east-west exchange of fauna (Fig. 10). Tectonically driven expansion of the Carpathian foreland basin towards the Eastern European platform may have generated or widened a connection towards the Central Paratethys (e.g. Kováč et al., 2007). East-west connectivity became more intense at mid-Konkian times. All middle Konkian (Sartaganian) mollusk species from the Eastern Paratethys (> 150 according to Studencka et al., 1998 and Iljina, 2003) are common with the upper Badenian (Kosovian) assemblages of the Central Paratethys. However, a connection to the Eastern Mediterranean, through the Lesser Caucasus and/or Mesopotamia, is also proposed to explain the diverse faunal associations in the southeastern parts (Mangyshlak, Usturt, Transcaucasian, North Iran) of the Eastern Paratethys basin (Iljina, 2003; Popov et al., 2006; Popov et al., 2015).

Recent $^{40}Ar/^{39}Ar$ dating of volcanic ash layers on top of the Badenian evaporites reveals that the BSC in the Central Paratethys had ended by 13.32 ± 0.07 Ma (De Leeuw et al., 2013; De Leeuw et al. under review). In the Carpathian foredeep of Romania, the marine Badenian (Kosovian) succession, corresponding to the late Badenian transgression (Kováč et al., 2007), is overlying the BSC gypsum and comprises faunal assemblages similar to the Serravallian of the Mediterranean (Kókay, 1985; Bartol et al., 2014).

This suggests that also the marine connection between the Central Paratethys and the Mediterranean was better functioning again during the Konkian/Kosovian time interval. The gateway between the Mediterranean and the Central Paratethys is thought to have been located in present-day Slovenia (Bartol et al., 2014), although some alternative hypotheses exist (Kováč et al., 2007).

In the Eastern Paratethys, the calcareous nannofossil assemblages of the upper part of the Konkian (Veselyankian) are marked by a sudden decrease in biodiversity and the rapid development of monospecific *Reticulofenestra pseudoumbilicus* with rare presence of *Rhabdosphaera poculi* (Golovina et al., 2004; Bratishko et al., 2015). In addition, euryhaline endemic mollusk (sub)species like *Acanthocardia andrussovi*, *Mactra basteroti konkensis*, *Parvivenus konkensis* and *Ervilia pusilla trigonula* become dominant. The bloom of *R. pseudoumbilicus* is very well documented in the Zelensky-Panagia section, but is also known from sections in the North Caucasus and the Transcaspian (Fig. 5). These nannofossil blooms, together with influxes of marine foraminifera, signal occasional exchanges between the Central and Eastern Paratethys seas. The inflow of relatively heavy marine waters from the Central Paratethys probably disturb (locally) the stratification of the Eastern Paratethys basin, creating nutrient rich upwelling currents that lead to nannoplankton blooms (Fig. 11B1).

6.3. The Volhynian: onset of a Paratethys pump - towards unified conditions

The Konkian/Volhynian boundary is placed at 50 m in the Zelensky-Panagia section at the level where the common marine nannofossil and foraminifera assemblages disappear from the record. The boundary is determined in the lower part of C5Ar.1r and is dated at an age of 12.65 Ma by extrapolation of constant sediment accumulation rates (Fig. 9). The Konkian/Volhynian boundary in the Eastern Paratethys has a similar age as the Badenian/Volhynian boundary in the Central Paratethys (Palcu et al., 2015). This suggests that connectivity changes between Eastern and Central Paratethys are simultaneously causing major paleoenvironmental changes at both sides of the gateway.

In Central Paratethys, the base of the Volhynian (lower substage of the Sarmatian) corresponds to the Badenian-Sarmatian Extinction Event (BSEE), the largest faunal turnover event in the Paratethys realm, including a full loss of coral, radiolarian and echinoid life forms from Central Paratethys (Harzhauser and Piller, 2007). It is recognized throughout the entire Central Paratethys and considered a synchronous event (Palcu et al., 2015).

At the age of 12.65 Ma, the oxygen isotope curves (Zachos et al., 2001; Holbourn et al., 2005) shows only a small fluctuations and the sea-level curve experiences only a small rise (Van De Wal et al., 2011) suggesting that global climate and sea level change were coupled with other events to trigger the BSEE. We conclude that tectonic widening and deepening of the Barlad Strait, coupled with a small sea-level increase, is the most likely cause for the event at the Konkian/Volhynian boundary. The Paratethyan system experiences a change of roles of its two main gateways, the Trans-Tethyan Strait persists but has a limited capacity of exchange while the Barlad Strait expands to become later, at the end of the Volhynian Stage, a proper seaway. The persistence of this connection during the Volhynian is evidenced by faunal assemblages that show similar characteristics east and west of the gateway (Studencka et al., 1998), indicating an effective water exchange between the two domains. Remarkably, the unification of Eastern and Central Paratethys at 12.65 Ma results in a highly controversial and poorly understood period with marine, brackish, and even fresh water fluxes, that make paleoenvironmental conditions highly variable (e.g. Piller and Harzhauser, 2005; Liu et al., 2017). Once the shifting chemistry had slowly stabilized, the sea became populated with the remarkably uniform “Sarmatian” endemic fauna. Nevertheless, shallow associations of Volhynian mollusks show some marked differences throughout the different Paratethys domains. Only in the Central Paratethys euryhaline marine species from genera like Loripes, Gari, Crassostrea, Gastrana and gastropods - Lunatia, Ocenebrina, Mitrella, Clavatula (hemistenohaline species, according to Kojumgieva, 1969) are observed.

The Kosovian and Konkian deposits contain significantly different faunal assemblages that reflect two distinct marine basins, each with its own salinity and water chemistry. These two basins had limited interactions through an ineffective strait. An increase of connectivity set a complex water exchange process in motion with devastating consequences for fauna in both Eastern and Central Paratethys. The water exchange mechanism characterized by stratified; density-driven flow has previously been proposed as an explanation for the environmental changes at the Badenian/Volhynian boundary (Palcu et al., 2015). The Zelensky-Panagia record confirms this pumping mechanism and allows reconstructing a timeline of events that marks the opening of a new gateway. The Konkian/Volhynian boundary can be considered equivalent to the initiation phase of exchange between the two basins with different salinity (Fig. 11.B2). This exchange mechanism occurs due to increase in the size of the gateway and adds a new dimension to the previous exchange dominated by the outflow of the Eastern Paratethys (that has a positive budget). A larger gateway triggers a density contrast and forces the heavier marine water from the Central Paratethys to sink into the deeper parts of Eastern Paratethys, effectively pumping the lighter (brackish) water from the Black Sea to flow out westwards over the gateway. There, it will probably remain on top of the marine waters, creating stratified conditions in the Central Paratethys. Similar to the configuration at present-day Gibraltar and Bosphorus, the density contrast between the two basins and the size of the connecting strait will accelerate the exchange speed (e.g. Marzocchi

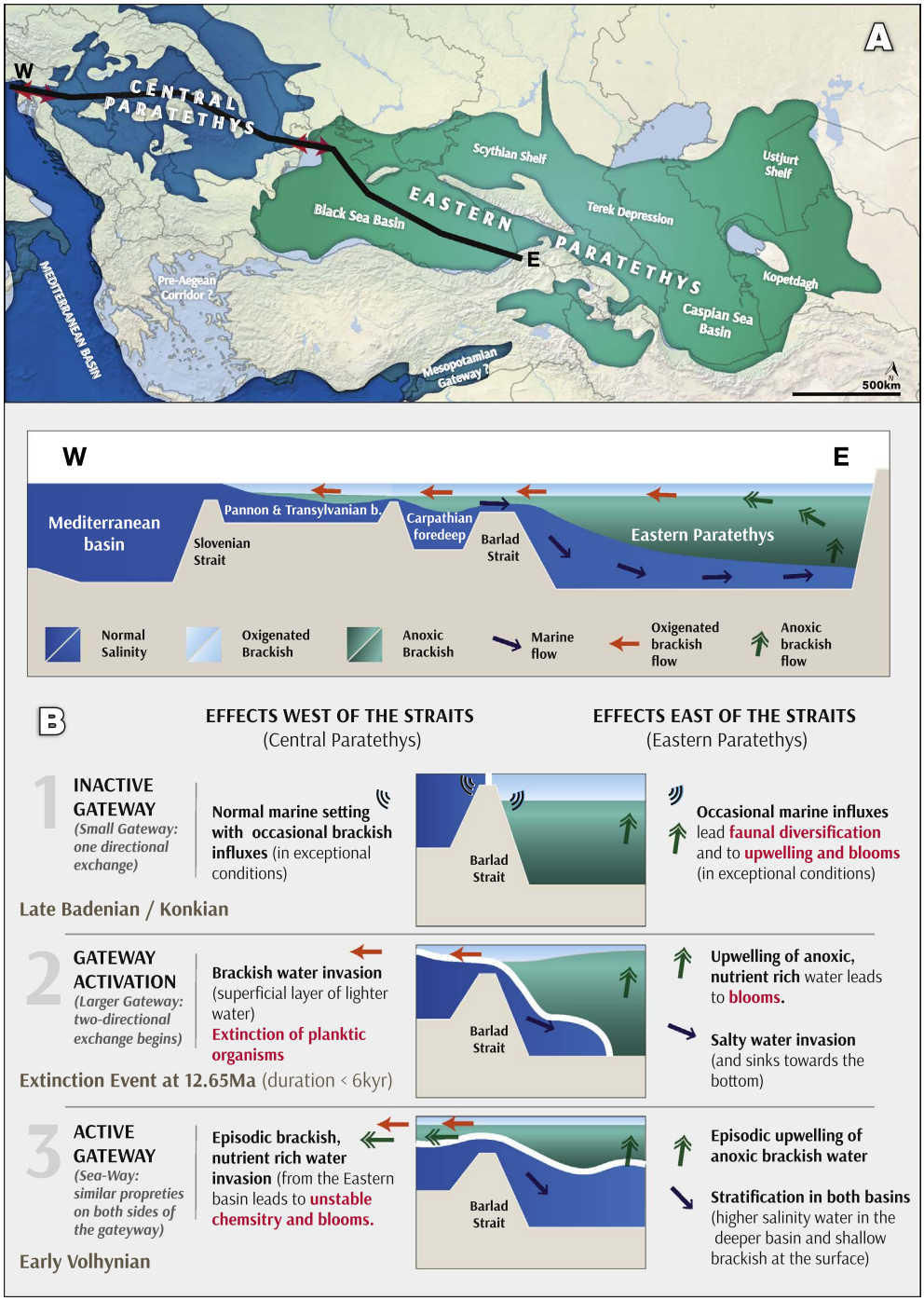

Fig. 11. (A) Paleogeographic configuration and circulation model responsible for the Badenian/Sarmatian Extinction Event (BSEE) and the Konkian/Volhynian Extinction. (B) Scenario of events at the end of the Konkian/Badenian stages; note the gradual opening of the Barlad gateway that allows a bidirectional mixing to be initiated.

et al., 2016). A second exchange phase (early Volhynian) occurs once the oxygenated light brackish water layer is spread in the whole system and thinned, giving place for the deeper anoxic water to upwell and cross the gateway into Central Paratethys (Fig. 11.B3). This heavier brackish-anoxic water, still lighter than the Central Paratethys water, is rich in nutrients and will fuel nutrient rich plumes that will cross the Barlad Strait, causing water stratification and unstable environmental conditions in the Central Paratethys, most likely depending on hydrological variations in the dominantly positive water budget of the Eastern Paratethys (e.g. Piller and Harzhauser, 2005; Liu et al., 2017). The observations of calcareous nannofossil blooms and mass development of diversified diatom floras in the Volhynian successions of the Polish Carpathian Foredeep are logically explained by such marine overflow waters from the Eastern Paratethys (Gaździcka, 2015).

7. Conclusions

We provide integrated magneto-biostratigraphic results from a continuous, 64 m long, sedimentary succession at the Taman peninsula on the northeastern coast of the Black Sea that straddles the uppermost Chokrakian - Karaganian - Konkian - early Volhynian interval of the Eastern Paratethys (Popov et al., 2016). The magnetostratigraphic record from the Zelensky-Panagia section consists of 5 normal and 4 reversed polarity intervals and its characteristic polarity pattern can be correlated to the C5ACn-C5An.2n interval of the GPTS. Our preferred correlation shows that the entire succession covers the time interval from 14.0 to 12.3 Ma. We date and describe three major paleoenvironmental changes, which can all be related to variations in the configuration of the paleo-straits that connected the Eastern Paratethys

with the Central Paratethys and the Mediterranean.

The Chokrakian/Karaganian boundary (13.8 Ma) is marked by the replacement of endemic marine Chokrakian fauna to low salinity and fresh water Karaganian taxa. A major sea level drop related to the global Mi3b cooling event isolated the Eastern Paratethys from the influences of the global ocean. The Karaganian successions are transgressive on the marginal regions of the Black Sea basin, indicating that the hydrological budget of the Eastern Paratethys was positive during this time interval. This created a unidirectional flow of brackish water into the easternmost basins of the Central Paratethys, which may have contributed to the formation of salt and gypsum during the BSC.

The Karaganian/Konkian transition (13.4 Ma) is marked by renewed marine influxes, which ended the isolated position of the Karaganian sea-lake of the Eastern Paratethys. Geodynamic changes in the gateway region resulted in the opening of a new gateway: the Barlad Strait north of Dobrogea. Faunal exchange with the Central Paratethys indicates a restricted two-way connectivity in the early Konkian, while east-west connectivity becomes more intense at mid-Konkian times.

The Konkian/Volhynian boundary (12.65 Ma) is marked by a sudden decrease in biodiversity and the disappearance of marine nannofossil and foraminifer assemblages. This indicates that connectivity changes between Eastern and Central Paratethys are simultaneously causing major paleoenvironmental changes at both sides of the Barlad Strait. We conclude that tectonic widening and deepening of the Barlad Strait generated an effective water exchange between the two domains. This increase of connectivity set a complex mixing process in motion whereby the heavier marine water from the Central Paratethys sank into the deeper parts of Eastern Paratethys, effectively pumping the lighter (brackish) water from the Black Sea to flow out westwards over the gateway. A second mixing phase (early Volhynian) occurred once the oxygenated light brackish water layer spread, giving place for the deeper anoxic water to upwell and cross the gateway into Central Paratethys.

Acknowledgements

Special thanks go to Irina Patina, Alexandra Rylova, Andrey Popkov, Alexander Guzhov, Jenea, Ira and Kubik for their help during the fieldwork. Special thanks go also to Eleonora Radionova, Valery Trubikhin for their support. Special thanks go to the people from Fort Hoofddijk, “the Forters” for their technical help and collegial support.

This work was financially supported by the Russian Foundation for Basic Research (14-05-00141 and 16-05-01032) and by the Netherlands Geosciences Foundation (ALW) (865.10.001) with support from the Netherlands Organization for Scientific Research (NWO) through the VICI grant of Wout Krijgsman.

References

Abels, H.A., Hilgen, F.J., Krijgsman, W., Kruk, R.W., Raffi, I., Turco, E., Zachariasse, W.J., 2005. Long-period orbital control on middle Miocene global cooling: integrated stratigraphy and astronomical tuning of the Blue Clay Formation on Malta. Paleoceanography 20 (4).

Andrusov, N.I., 1917. Konkian Horizon (Pholada beds)//Proc. geol. and mineral. mus. AS. Vol. 2. pp. 167–261 ess.6. (In Russian).

Báldi, K., Veledits, F., Ćorić, S., Lemberkovics, V., Lőrincz, K., Shevelev, M., 2015. New discovery of mid-Miocene (Badenian) evaporites inside the Carpathian arc – possible implications for global climate change and Paratethys salinity. Neogene of the Paratethyan Region - 6th workshop on the Neogene of Central and South-Eastern Europe - Hungarian Geological Society978-963-8221-57-5pp. 16.

Báldi, K., Velledits, F., Ćorić, S., Lemberkovics, V., Lőrincz, K., Shevelev, M., 2017. Discovery of the Badenian evaporites inside the Carpathian Arc: implications for global climate change and Paratethys salinity. Geol. Carpath. 68 (3), 193–206. http://dx.doi.org/10.1515/geoca-2017-0015.

Bartol, M., Mikuž, V. and Horvat, A., (2014). "Palaeontological evidence of communication between the Central Paratethys and the Mediterranean in the late Badenian/early Serravalian." Palaeogeogr. Palaeoclimatol. Palaeoecol. 394(0): 144–157.

Bethoux, J.P., Pierre, C., 1999. Mediterranean functioning and sapropel formation: respective influences of climate and hydrological changes in the Atlantic and the Mediterranean. Mar. Geol. 153 (1), 29–39.

Bicchi, E., Ferrero, E., and Gonera, M., (2003), Palaeoclimatic interpretation based on Middle Miocene planktonic foraminifera: the Silesia Basin (Paratethys) and Monferrato (Tethys) records: Palaeogeogr. Palaeoclimatol. Palaeoecol., v. 196, p. 265–303, doi: https://doi.org/10.1016/S0031-0182(03)00368-7.

Bogdanovich, A.K., 1965. Stratigraphic and facies distribution of Foraminifera in the Miocene of the West Caucasus and issues of their genesis., Moscow: Nedra. In: Proc. Krasnodar. Phil. VNIIneft., Krasnodar, N 16pp. 300–350 (In Russian).

ter Borgh, M., Vasiliev, I., Stoica, M., Knežević, S., Matenco, L., Krijgsman, W., Rundić, L., Cloetingh, S., 2013. The isolation of the Pannonian basin (Central Paratethys): New constraints from magnetostratigraphy and biostratigraphy. Glob. Planet. Chang. 103 (1), 99–118.

Bratishko A., Schwarzhans W., Reichenbacher B., Vernyhorova Y., Coric S., (2015), Fish otoliths from the Konkian (Miocene, early Serravallian) of Mangyshlak (Kazakhstan): testimony to an early endemic evolution in the Eastern Paratethys, Palaeontol. Z., v 89, n-4, pp. 839-889.

Bukowski, K., de Leeuw, A., Gonera, M., Kuiper, K.F., Krzywiec, P., Peryt, D., 2010. Badenian tuffite levels within the Carpathian orogenic front (Gdów-Bochnia area, Southern Poland): radio-isotopic dating and strati graphic position. Geological Quarterly 54 (4), 449–464.

Chiriac, M., 1970. Raspindirea si faciesurile Tortonianului in Dobrogea de sud, Dari de seama ale sedintelor. Institutul Geologic 56 (4), 89–112.

Cramp, A., O'Sullivan, G., (1999), Neogene sapropels in the Mediterranean: a review, Mar. Geol., v. 153, p. 11–28.

De la Vara, A., van Baak, C.G.C., Marzocchi, A., Arjen Grothe, A., Meijer, P.Th., 2016. Quantitative analysis of Paratethys sea level change during the Messinian salinity crisis. Mar. Geol. 379 (2016), 39–51. http://dx.doi.org/10.1016/j.margeo.2016.05.002.

De Leeuw, A., Bukowski, K., Krijgsman, W., Kuiper, K.F., 2010. Age of the Badenian salinity crisis; impact of Miocene climate variability on the circum-mediterranean region. Geology 38 (8), 715–718.

De Leeuw, A., Filipescu, S., Maţenco, L., Krijgsman, W., Kuiper, K., Stoica, M., 2013. Paleomagnetic and chronostratigraphic constraints on the middle to late Miocene evolution of the Transylvanian basin (Romania): implications for central Paratethys stratigraphy and emplacement of the Tisza-Dacia plate. Glob. Planet. Chang. 103 (1), 82–98.

De Leeuw, A., Tulbure, M., Kuiper, K., Melinte-Dobrinescu, M., Stoica, M., Krijgsman, W., 2017. New $^{40}Ar/^{39}Ar$ and magnetostratigraphic constraints on the termination of the Badenian salinity crisis: evidence for tectonic improvement of basin interconnectivity in Southern Europe. In: Global and Planetary Change, (in press).

Dela Pierre, F., Natalicchio, M., Ferrando, S., Giustetto, R., Birgel, D., Carnevale, G., Gier, S., Lozar, F., Marabello, D., Peckmann, J., 2015. Are the large filamentous microfossils preserved in Messinian gypsum colorless sulfide-oxidizing bacteria? Geology 43 (10), 855–858.

Dzhanelidze, O.I., 1970. Foraminifera fom the Lower and the Middle Miocene of Georgia, Tbilisi: Metsniereba. 172 p. (in Russian).

Evans, N.P., Turchyn, A.V., Gázquez, F., Bontognali, T.R.R., Chapman, H.J., Hodell, D.A., 2015. Coupled measurements of δ18O and δD of hydration water and salinity of fluid inclusions in gypsum from the Messinian Yesares Member, Sorbas Basin (SE Spain). Earth Planet. Sci. Lett. 430, 499–510. ISSN 0012-821X. https://doi.org/10.1016/j.epsl.2015.07.071.

Flecker, R., Krijgsman, W., Capella, W., de Castro Martíns, C., Dmitrieva, E., Mayser, J.P., Marzocchi, A., Modestu, S., Ochoa, D., Simon, D., Tulbure, M., van den Berg, B., van der Schee, M., de Lange, G., Ellam, R., Govers, R., Gutjahr, M., Hilgen, F., Kouwenhoven, T., Lofi, J., Meijer, P., Sierro, F.J., Bachiri, N., Barhoun, N., Alami, A.C., Chacon, B., Flores, J.A., Gregory, J., Howard, J., Lunt, D., Ochoa, M., Pancost, R., Vincent, S., Yousfi, M.Z., 2015. Evolution of the Late Miocene Mediterranean–Atlantic gateways and their impact on regional and global environmental change. Earth-Sci. Rev. 150, 365–392.

Gaździcka, E., 2015. Middle Miocene calcareous nannofossils and diatoms from the Busko and Kazimierza Wielka area (northern part of the Carpathian Foredeep). Biuletyn Państwowego Instytutu Geologicznego (0867-6143) 461, 153–177.

Golovina, L., Goncharova, I., Rostovtseva, Yu., (2004), New data on biostratigraphy (nannoplankton, molluscs) and lithology of the Middle Miocene of Taman Peninsula and the Western Caucasus. Stratigr. Geol. Correl., V. 12. N 6. P. 103–112.

Goncharova, Karaganian, I.A., 1975. In: Steininger, Nevesskaya (Ed.), Stratotypes of Mediterranean Stages, Bratislava, VEDA. 171. pp. 233–234.

Gonera, M., Peryt, T.M., Durakiewicz, T., 2000. Biostratigraphical and palaeoenvironmental implications of isotopic studies (^{18}O, ^{13}C) of middle Miocene (Badenian) foraminifers in the Central Paratethys. Terra Nova 12, 231–238. http://dx.doi.org/10.1046/j.1365-3121.2000.00303.x.

Gradinaru, E., 2015. Badenian rocky near-shore facies in Dobrogea - a new finding in the Capidava area. In: Abstracta and Field Tripe Guide. Conference Paper: 10th Romanian Symposium on Paleontology, At Cluj-Napoca, Romania.

Handler, R., Ebner, F., Neubauer, F., Bojar, A.V., Hermann, S., 2006. $^{40}Ar/^{39}Ar$ dating of Miocene tuffs from the Styrian part of the Pannonian Basin: an attempt to refine the basin stratigraphy. Geol. Carpath. 57 (6), 483–494.

Harzhauser, M., Piller, W.E., 2004. Integrated stratigraphy of the Sarmatian (Upper Middle Miocene) in the western Central Paratethys. Stratigraphy 1 (1), 65–86.

Harzhauser, M., Piller, W.E., 2007. Benchmark data of a changing sea — Palaeogeography, Palaeobiogeography and events in the Central Paratethys during the Miocene. Palaeogeogr. Palaeoclimatol. Palaeoecol. 253 (1–2), 8–31.

Hilgen, F.J., Abels, H.A., Iaccarino, S., Krijgsman, W., Raffi, I., Sprovieri, R., Turco, E., Zachariasse, W.J., 2009. The global stratotype section and point (GSSP) of the serravallian stage (Middle Miocene). Episodes 32 (3), 152–166.

Hilgen, F.J., Lourens, L.J., Van Dam, J.A., Beu, A.G., Boyes, A.F., Cooper, R.A., Krijgsman, W., Ogg, J.G., Piller, W.E., Wilson, D.S., 2012. The Neogene Period. The Geologic Time Scale 2012. 1–2. pp. 923–978.

Hohenegger, J., Rögl, F., Ćorić, S., Pervesler, P., Lirer, F., Roetzel, R., Scholger, R., Stingl, K., 2009. The Styrian Basin: a key to the Middle Miocene (Badenian/Langhian) Central Paratethys transgressions. Aust. J. Earth Sci. 102 (1), 102–132.

Holbourn, A., Kuhnt, W., Schulz, M., Erlenkeuser, H., 2005. Impacts of orbital forcing and

atmospheric carbon dioxide on Miocene ice-sheet expansion. Nature 438 (7067), 483–487.
Holbourn, A., Kuhnt, W., Clemens, S.C., Prell, W.L., Andersen, N., 2013. Stable carbon and oxygen isotope ratios of benthic foraminifera from ODP Site 184-1146. doi:10.1594/PANGAEA.825478, In supplement to: Holbourn, A., Kuhnt, W., Clemens, S. C., Prell, W. L., Andersen, N., (2013): Middle to late Miocene stepwise climate cooling: Evidence from a high-resolution deep water isotope curve spanning 8 million years. Paleoceanography 28, 1–12. http://dx.doi.org/10.1002/2013PA002538.
Iljina, L.B., 2003. Zoogeography of Konkian (Middle Miocene) bivalves and gastropods. Paleontol. J. 2, 13–20.
John, C.M., Karner, G.D., Browning, E., Leckie, R.M., Mateo, Z., Carson, B., Lowery, C., 2011. Timing and magnitude of Miocene eustasy derived from the mixed siliciclastic-carbonate stratigraphic record of the northeastern Australian margin. Earth Planet. Sci. Lett. 304 (2011), 455–467. http://dx.doi.org/10.1016/j.epsl.2011.02.013.
Kirschvink, J.L., 1980. The least-squares line and plane and the analysis of palaeomagnetic data. Geophys. J. Roy. Astron. Soc. 62 (3), 699–718.
Kókay, J., 1985. Central and Eastern Paratethyan interrelations in the light of Late Badenian salinity conditions. In: Geologica Hungarica, Series Palaeontologica 48. pp. 9–95 Budapest.
Kováč, M., Andreyeva-Grigorovich, A., Bajraktarević, Z., Brzobohatý, R., Filipescu, S., Fodor, L., Harzhauser, M., Nagymarosy, A., Oszczypko, N., Pavelić, D., Rögl, F., Saftić, B., Sliva, L., Studencka, B., 2007. Badenian evolution of the Central Paratethys Sea: Paleogeography, climate and eustatic sea-level changes. Geol. Carpath. 58 (6), 579–606.
Krasheninnikov, V.A., 1959. Foraminifera. In: Atlas Middle Miocene fauna of the North Caucasus and the Crimea., M.: Gostoptekhizdat, pp. 15–103 (In Russian).
Krijgsman, W., Fortuin, A. R., Hilgen, F. J., and Sierro, F. J., (2001), Astrochronology for the Messinian Sorbas basin (SE Spain) and orbital (precessional) forcing for evaporite cyclicity: Sediment. Geol., v. 140, no. 1–2, p. 18.
Krijgsman, W., Stoica, M., Vasiliev, I., Popov, V.V., 2010. Rise and fall of the Paratethys Sea during the Messinian salinity crisis. Earth Planet. Sci. Lett. 290 (1–2), 183–191.
Liu, S., Krijgsman, W., Dekkers, M.J., Palcu, D.V., 2017. Early diagenetic greigite as an indicator of paleosalinity changes in the middle Miocene Paratethys Sea of central Europe. Geochem. Geophys. Geosyst. 18, 2634–2645. http://dx.doi.org/10.1002/2017GC006988.
Magyar, I., Geary, D.H., Müller, P., 1999. Paleogeographic evolution of the Late Miocene Lake Pannon in Central Europe. Palaeogeogr. Palaeoclimatol. Palaeoecol. 147 (3–4), 151–167.
Mandic, O., de Leeuw, A., Vuković, B., Krijgsman, W., Harzhauser, M., Kuiper, K.F., 2011. Palaeoenvironmental evolution of Lake Gacko (Southern Bosnia and Herzegovina): impact of the Middle Miocene Climatic Optimum on the Dinaride Lake System. Palaeogeogr. Palaeoclimatol. Palaeoecol. 299 (3–4), 475–492.
Marzocchi, A., Flecker, R., Baak, C.G.K., Lunt, D.J., Krijgsman, W., 2016. Mediterranean outflow pump: an alternative mechanism for the Lago-mare and the end of the Messinian Salinity Crisis. Geology 44 (7), 523.
Merklin, R.L., 1953. The stages of Konkian basin development in the Miocene of the southern USSR. Bulletin Moskovskogo obchsestva ispytateley prirody, otdelenie geologii 28 (3), 89–91 (in Russian).
Michajlovskij, G.P., 1909. Geological study in South-Western Bessarabia. Proceedings of the Geological Committee 28 (6), 477–508.
Mullender, T.A.T., van Velzen, A.J., Dekkers, M.J., 1993. Continuous drift correction and separate identification of ferrimagnetic and paramagnetic contributions in thermomagnetic runs. Geophys. J. Int. 114, 663–672.
Natalicchio, M., Dela Pierre, F., Lugli, S., Lowenstein, T. K., Feiner, S. J., Ferrando, S., Manzi, V., Roveri, M., and Clari, P., (2014), Did Late Miocene (Messinian) gypsum precipitate from evaporated marine brines? Insights from the Piedmont Basin (Italy): Geology, v. 42, p. 179–182.
Nevesskaya, L., Goncharova, I.A., Ilyina, L., 2005a. Types of Neogene marine and non-marine basins exemplified by the Eastern Paratethys. Paleontol. J. 39 (3), 227–235.
Nevesskaya, L.A., Kovalenko, E.I., Beluzhenko, E.V., 2005b. Regional stratigraphic scheme of the Neogene of southern European part of Russia. In: Stratigrafiya, regionalnaya geologiya i tektonika. 4. pp. 47–59 (in Russian).
Oldfield, F., 2012. Mud and magnetism: records of late Pleistocene and Holocene environmental change recorded by magnetic measurements. J. Paleolimnol. 49 (3).
Palcu, D., Tulbure, M., Bartol, M., Kouwenhoven, T.J., Krijgsman, W., 2015. The Badenian–Sarmatian extinction event in the Carpathian foredeep basin of Romania: paleogeographic changes in the Paratethys domain. Global Planet. Change 133, 346–358.
Paramonova N.P., Belokrys L.S., (1972), On volume of the Sarmatian stage//Bull. MOIP. Geol. Depart., V. 72, Ess. 3. P. 36–47 (in Russian).
Paulissen, W., Luthi, S., Grunert, P., Čorić, S., Harzhauser, M., 2011. Integrated high-resolution stratigraphy of a Middle to Late Miocene sedimentary sequence in the central part of the Vienna Basin. Geol. Carpath. 62 (2), 155–169.
Peryt, T.M., 2006. The beginning, development and termination of the Middle Miocene Badenian salinity crisis in Central Paratethys. Sediment. Geol. 188-189, 379–396.
Peryt, T.M., Peryt, D., Jasionowski, M., Poberezhskyy, A.V., Durakiewicz, T., 2004. Post-evaporitic restricted deposition in the Middle Miocene Chokrakian-Karaganian of East Crimea (Ukraine). Sediment. Geol. 170 (1–2), 21–36.
Piller, W.E., Harzhauser, M., 2005. The myth of the brackish Sarmatian Sea. Terra Nova 17 (5), 450–455.
Pinchuk, T.N., 2006. Western Caucasus and Ciscaucasia (Oligocene and Neogene), Practical guide on microfauna USSR. Cenozoic Foraminifera S.-Pb., Nedra. pp. 91–98 (in Russian).
Popov, S.V., et al., 2004. Lithological–paleogeographic maps of Paratethys. In: CFS Courier Forschungsinstitut Senckenberg, pp. 1–46.
Popov, S.V., Shcherba, I.G., Ilyina, L.B., Nevesskaya, L.A., Paramonova, N.P., Khondkarian, S.O., Magyar, I., 2006. Late Miocene to Pliocene palaeogeography of the Paratethys and its relation to the Mediterranean. Palaeogeogr. Palaeoclimatol. Palaeoecol. 238 (1–4), 91–106.
Popov, S., Vernigorova, Yu., Goncharova, I., Pinchuk, T., Yu, Gladenkov, 2009. Stratigraphy of the Middle - Upper Miocene sections of the Taman by mollusk and foraminifers. In: Actual Problems of Neogene and Quater. Strat. and their discussion of 33 Int. Geol. Congresspp. 96–100 (in Russian).
Popov S.V., Golovina L.A., Jafarzadeh M., Goncharova I.A., (2015) Eastern Paratethys Miocene deposits, mollusks and nannoplankton of the Northern Iran//Neogene of the Paratethyan Region, 6 workshop on Neogene of Central and SE Europe, 31 May – 3 June 2015, Orfu, Hungary. P. 71-72.
Popov, S.V. et al. (2016). “Paleontology and stratigraphy of the Middle – Upper Miocene of Taman Peninsula. Part 1. Description of key-sections and benthic fossil groups (Eds. Popov S.V., Golovina L.A.)”, Paleontol. Journ. Suppl. Ser., Vol. 50, No. 10, 168 p.
Radionova E.P., Golovina L.A., Filippova N.Yu., Trubikhin V.M., Popov S.V., Goncharova I.A., Vernigorova Yu.V., Pinchuk T.N., (2012), Middle-Upper Miocene stratigraphy of the Taman Peninsula, Eastern Paratethys//Central Europ. J. Geosci. V. 4, № 1. P. 188–204. DOI: https://doi.org/10.2478/s13533-011-0065-8
Rögl, F., 1998. Palaeogeographic considerations for Mediterranean and Paratethys seaways (Oligocene to Miocene). Ann. Naturhist. Mus. Wien 99 A (A), 279–310.
Rogl, F., 1999. Mediterranean and Paratethys. Facts and hypotheses of an Oligocene to Miocene paleogeography (short overview). Geol. Carpath. 50 (4), 339–349.
Roveri, M., Flecker, R., Krijgsman, W., Lofi, J., Lugli, S., Manzi, V., Sierro, F.J., Bertini, A., Camerlenghi, A., DeLange, G., Hilgen, F.J., Hübscher, C., Govers, R., Meijer, P.Th., Stoica, M., 2014. The Messinian salinity crisis: past and future of a great challenge for marine sciences. Mar. Geol. 352, 25–58. http://dx.doi.org/10.1016/j.margeo.2014.02.002.
Rybkina, A.I., Kern, A.N., Rostovtseva, Yu.V., 2015. New evidence of the age of the lower Maeotian substage of the Eastern Paratethys based on astronomical cycles. Sediment. Geol. 330, 122–131. http://dx.doi.org/10.1016/j.sedgeo.2015.10.003.
Sant, K., Palcu, D.V., Mandic, O., Krijgsman, W., 2017. Changing seas in the Early-Middle Miocene of Central Europe. Terra Nova. http://dx.doi.org/10.1111/ter.12273.
Selmeczi, I., Lantos, M., Bohn-Havas, M., Nagymarosy, A., Szegő, E., 2012. Correlation of bio-and magnetostratigraphy of Badenian sequences from western and northern Hungary. Geol. Carpath. 63 (3), 219–232.
Śliwiński, M., Bábel, M., Nejbert, K., Olszewska-Nejbert, D., Gásiewicz, A., Schreiber, B.C., Benowitz, J.A., Layer, P., 2012. Badenian-Sarmatian chronostratigraphy in the Polish Carpathian Foredeep. Palaeogeogr. Palaeoclimatol. Palaeoecol. 326-328, 12–29.
Sokolov, N. A., (1899). Layers with Venus konkensis at Konka River, Proc. Geol. Committee, Vol. 9. № 5. (96 p).
Stoica, M., Krijgsman, W., Fortuin, A.R., Gliozzi, E., 2016. Paratethyan ostracods in the Spanish Lago-Mare: more evidence for interbasinal exchange at high Mediterranean sea level. Palaeogeogr. Palaeoclimatol. Palaeoecol. 441, 854–870.
Studencka, B., Gontsharova, I.A., Popov, S.V., 1998. The bivalve faunas as a basis for reconstruction of the Middle Miocene history of the Paratethys. Acta Geol. Pol. 48 (3), 285–342.
Suess E., (1866). Untersuchungen über den Charakter der österreichischen Tertiärablagerungen. II. Über den Charakterder der brackischen Stufe oder der Cerithienschichten, Sitzber. Osterr. Acad. Wiss. math.-naturwiss, Wien. Kl.. Bd. 54. S. 218–357.
Szuromi-Korecz, A., Selmeczi, I., 2015. Middle Miocene evaporites from borehole successions in Hungary. Neogene of the Paratethyan Region - 6th workshop on the Neogene of Central and South-Eastern Europe - Hungarian Geological Society978-963-8221-57-5pp. 91.
Thompson, R., Oldfield, F., 1986. Environmental Magnetism. Allen and Unwin, London.
Van De Wal, R.S.W., et al., 2011. Reconstruction of a continuous high-resolution CO 2 record over the past 20 million years. Clim. Past 7 (4), 1459–1469.
Vasiliev, I., de Leeuw, A., Filipescu, S., Krijgsman, W., Kuiper, K., Stoica, M., Briceag, A., 2010. The age of the Sarmatian-Pannonian transition in the Transylvanian Basin (Central Paratethys). Palaeogeogr. Palaeoclimatol. Palaeoecol. 297 (1), 54–69.
Vasiliev, I., Iosifidi, A.G., Khramov, A.N., Krijgsman, W., Kuiper, K., Langereis, C.G., Popov, V.V., Stoica, M., Tomsha, V.A., Yudin, S.V., 2011. Magnetostratigraphy and radio-isotope dating of upper Miocene-lower Pliocene sedimentary successions of the Black Sea Basin (Taman Peninsula, Russia). Palaeogeogr. Palaeoclimatol. Palaeoecol. 310 (3–4), 163–175.
Vernigorova, Yu.V., 2009. The Karaganian and Konkian regional stage of the Eastern Paratethys: questions of their stratigraphic volume and stratigraphic autonomy. Geologichnyi Journal 2, 34–47 (in Russian).
Vernigorova, Yu.V., Golovina, L., Goncharova, I., 2006. On the characterization of Konkian deposits of the Taman Peninsula. In: Proc. Inst. Geol. Sci. NAS Ukrainepp. 231–242 (In Russian).
Vernyhorova, Yu.V., 2015. The criteria for stratigraphy of the Konkian sediments of the Eastern Paratethys based on molluscs and Foraminifera. Kiyv. Geologichyi zhurnal 4, 77–86 (in Russian).
Zachos, J., Pagani, M., Sloan, L., Thomas, E., and Billups, K., 2001, Trends, rhythms, and aberrations in global climate 65 Ma to present: Science, v. 292, p. 686–693, doi:https://doi.org/10.1126/science.1059412.
Zijderveld, J.D.A., 1967. AC demagnetization of rocks: Analysis of results. In: Methods in Paleomagnetism, pp. 254–286.